



Call: H2020-SC5-2014-two-stage

Topic: SC5-01-2014

PRIMAVERA

Grant Agreement 641727



PRocess-based climate sIMulation: AdVances in high resolution modelling and European climate Risk Assessment

Deliverable D2.1

Assessment of the benefits of increased resolution on the North Atlantic Ocean dynamics and processes and the Arctic sea ice conditions and their robustness across the pre-PRIMAVERA multi-model ensemble

Deliverable Title	<i>Assessment of the benefits of increased resolution on the North Atlantic Ocean dynamics and processes and the Arctic sea ice conditions and their robustness across the pre-PRIMAVERA multi-model ensemble listed in milestone MS1</i>
Brief Description	<i>This deliverable contains an assessment of the impact of model resolution on ocean and sea ice processes in the North Atlantic and Arctic regions using pre-PRIMAVERA climate model simulations</i>
WP number	2
Lead Beneficiary	UCL
Contributors	<p><i>David Docquier (UCL)</i> <i>Torben Koenigk (SMHI)</i> <i>Eleftheria Exarchou (BSC)</i> <i>François Massonnet (UCL / BSC)</i> <i>Thierry Fichefet (UCL)</i> <i>Antoine Barthélémy (UCL)</i> <i>Ramon Fuentes Franco (SMHI)</i> <i>Martin Evaldsson (SMHI)</i> <i>Mihaela Caian (NMA / SMHI)</i> <i>Neven Fuckar (BSC)</i> <i>Panos Athanasiadis (CMCC)</i> <i>Malcolm Roberts (MET OFFICE)</i> <i>Rein Haarsma (KNMI)</i> <i>Chunxue Yang (CNR)</i> <i>Susanna Corti (CNR)</i> <i>Johann Jungclaus (MPG)</i> <i>Jin-Song von Storch (MPG)</i> <i>Katja Lohmann (MPG)</i> <i>Dian Putrasahan (MPG)</i> <i>Sebastian Milinski (MPG)</i> <i>Emilia Sanchez-Gomez (CERFACS)</i> <i>Rym Msadek (CERFACS)</i> <i>Jeremy Grist (NERC)</i> <i>Adrian New (NERC)</i> <i>Simon Josey (NERC)</i> <i>Tido Semmler (AWI)</i> <i>Dmitry Sein (AWI)</i> <i>Jan Hegewald (AWI)</i> <i>Marie-Estelle Demory (UREAD)</i> <i>Alexander Baker (UREAD)</i> <i>Reinhard Schiemann (UREAD)</i> <i>Benoit Vanniere (UREAD)</i> <i>Pier Luigi Vidale (UREAD)</i></p>
Creation Date	16/01/2017
Version Number	3
Version Date	23/02/2017
Deliverable Due Date	01/02/2017
Actual Delivery Date	23/02/2017

Nature of the Deliverable	<i>R - Report</i> <i>P - Prototype</i> <i>D - Demonstrator</i> <i>O - Other</i>
Dissemination Level/ Audience	<i>PU - Public</i> <i>PP - Restricted to other programme participants, including the Commission services</i> <i>RE - Restricted to a group specified by the consortium, including the Commission services</i> <i>CO - Confidential, only for members of the consortium, including the Commission services</i>

Version	Date	Modified by	Comments
Version 1	10/02/2017	David Docquier	Including contributions from every partner
Version 2	15/02/2017	David Docquier	Including comments and corrections from T. Koenigk and E. Exarchou
Version 3	23/02/2017	David Docquier	Including comments and corrections from every partner

Table of Contents

1. Executive Summary.....	4
2. Project Objectives.....	5
3. Detailed Report.....	6
3.1 North Atlantic Ocean.....	6
3.2. Arctic sea ice.....	21
3.3. Atmosphere.....	28
3.4. Peer-reviewed articles arising from the project.....	37
3.5. Other references.....	38
4. Lessons Learnt.....	39
5. Links Built.....	40



1. Executive Summary

The focus of this deliverable is on the impact of increased horizontal resolution on oceanic and sea ice related processes in the North Atlantic and Arctic regions. Partners have investigated processes in the North Atlantic and Arctic regions which potentially affect climate variations over Europe. In addition, analysis of high resolution on atmospheric processes in the North Atlantic region has also been undertaken.

Diagnostics have been developed in collaboration with WP1 and applied to the pre-PRIMAVERA data on JASMIN. The compilation of results in this deliverable has been possible thanks to an important number of discussions (e.g. at the PRIMAVERA Second General Assembly at KNMI in November 2016), teleconferences and written comments on the PRIMAVERA wiki pages.

The effect of resolution on North Atlantic and Arctic processes cannot be summarized by one single result but rather by a wide range of results depending on the theme that is studied. In other words, increasing the resolution can lead to the improvement of a specific process, while it does not necessarily improve another process. Knowing the minimal resolution that is needed to accurately compute a process and the resolution threshold over which there is no improvement are crucial. Furthermore, for certain processes, it is also very important to isolate the effect of the ocean resolution from the atmosphere resolution. This deliverables aims at providing some key results arising from the analysis of pre-PRIMAVERA model outputs, which will help guiding a careful analysis of PRIMAVERA simulations with respect to horizontal resolution.

This deliverable includes a detailed report of the main results achieved (Section 3) grouped into three main components, i.e. North Atlantic Ocean (sub-Section 3.1), Arctic sea ice (sub-Section 3.2) and the atmosphere (sub-Section 3.3). For each of these three sub-sections, results are present by theme with the responsible partner in brackets. The reader can go to the end of these three sub-sections to find a list of key findings related to the impact of resolution. Section 3 also contains a list of peer-reviewed articles arising from the project (published, submitted or in preparation, see sub-Section 3.4) as well as a list of other references used to carry out the work (sub-Section 3.5). Section 4 presents key positive, negative and neutral lessons coming from the work undertaken. Finally, Section 5 shows some links created by WP2 with other PRIMAVERA work packages as well as other projects.

2. Project Objectives

With this deliverable, the project has contributed to the achievement of the following objectives (DOA, Part B Section 1.1) WP numbers are in brackets:

No.	Objective	Yes	No
A	To develop a new generation of global high-resolution climate models. (3, 4, 6)		
B	To develop new strategies and tools for evaluating global high-resolution climate models at a process level, and for quantifying the uncertainties in the predictions of regional climate. (1, 2, 5, 9, 10)		
C	To provide new high-resolution protocols and flagship simulations for the World Climate Research Programme (WCRP)'s Coupled Model Intercomparison Project (CMIP6) project, to inform the Intergovernmental Panel on Climate Change (IPCC) assessments and in support of emerging Climate Services. (4, 6, 9)		
D	To explore the scientific and technological frontiers of capability in global climate modelling to provide guidance for the development of future generations of prediction systems, global climate and Earth System models (informing post-CMIP6 and beyond). (3, 4)		
E	To advance understanding of past and future, natural and anthropogenic, drivers of variability and changes in European climate, including high impact events, by exploiting new capabilities in high-resolution global climate modelling. (1, 2, 5)		
F	To produce new, more robust and trustworthy projections of European climate for the next few decades based on improved global models and advances in process understanding. (2, 3, 5, 6, 10)		
G	To engage with targeted end-user groups in key European economic sectors to strengthen their competitiveness, growth, resilience and ability by exploiting new scientific progress. (10, 11)		
H	To establish cooperation between science and policy actions at European and international level, to support the development of effective climate change policies, optimize public decision making and increase capability to manage climate risks. (5, 8, 10)		

3. Detailed Report

For each of the three main components, namely North Atlantic Ocean (sub-Section 3.1), Arctic sea ice (sub-Section 3.2) and the atmosphere (sub-Section 3.3), the main results are grouped by themes. The responsible partner for each theme is put in brackets.

3.1. North Atlantic Ocean

3.1.1. Ocean heat transport (NERC)

The resolution dependence of Atlantic meridional ocean heat transport has been examined in pre-PRIMAVERA multi-model ensemble. Further work is continuing to understanding the changes in air-sea heat fluxes that are associated with these changes in ocean heat transport.

The pre-PRIMAVERA ensemble analyzed in this context consists of pairs of runs with different types of resolution changes. Specifically:

- 1) A changing atmospheric resolution with constant $1/4^{\circ}$ ocean resolution (UKMO-HadGEM3-GC2: N96 ORCA025; N216 ORCA025; N512 ORCA025).
- 2) A constant atmospheric resolution with ocean resolution increasing from 1° to $1/4^{\circ}$ (CMCC-CM2: 192x288 ORCA1; 192x288 ORCA025).
- 3) An increasing atmospheric resolution together with ocean resolution increasing from 1° to $1/4^{\circ}$ (EC-Earth3.1: T255 ORCA1; T511 ORCA025).

In addition, there are two pairs of higher resolution runs:

- 4) Increasing atmospheric resolution with ocean resolution increasing from $1/4^{\circ}$ to $1/12^{\circ}$ (HadGEM3-GC2.1: N216 ORCA025; N512 ORCA12).
- 5) A constant atmospheric resolution with ocean resolution increasing from $\sim 0.4^{\circ}$ to $\sim 0.1^{\circ}$ (MPI-ESM: T63-TP04; T63-TP6M).

Atlantic meridional ocean heat transport in the 1° or $1/4^{\circ}$ models tends toward the low end of the observational error range (Fig. 1). Increasing the atmospheric resolution from N96 to N216 and from N216 to N512 appears to make little difference to the Atlantic heat transport (Fig. 1, top panel). Increasing the ocean resolution from 1° to $1/4^{\circ}$ while keeping the atmosphere at 192x288 resolution results in a significant increase in heat transport in the North Atlantic (Fig. 1, middle panel). Based on the 26°N section this increase is more in accord with observations. Increasing the ocean resolution from 1° to $1/4^{\circ}$ while increasing the atmosphere from T255 to T511 results in a more significant increase in ocean heat transport at all latitudes north of 15°N (Fig. 1, bottom panel).

Bearing in mind that model pairs (2) and (3) result in increased ocean heat transport, there must also be changes in the surface heat fluxes. Similar surface flux changes to (2) and (3) include an increase in latent heat and longwave ocean heat loss in the mid-high latitude North Atlantic (Fig. 2). However (2) and (3) have different changes in solar radiation, with (2) having less downward shortwave flux at the poles and more in the tropics, whereas (3) has generally more downward shortwave radiation. For the higher resolution models (4) and (5) an increase in ocean heat transport is primarily accompanied by an increase in mid-high latitude oceanic latent heat loss (not shown).

Resolution dependence of zonal Atlantic heat transport in pre-Primavera runs

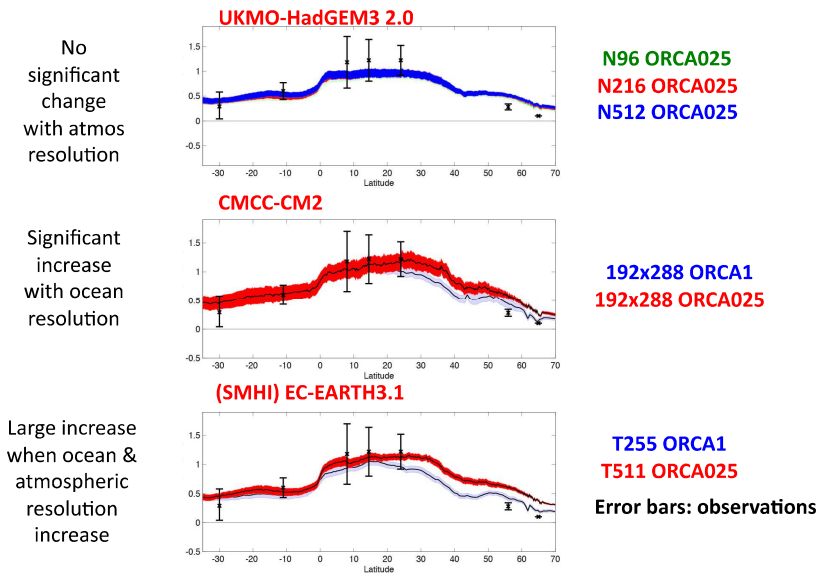


Figure 1: Zonally integrated Atlantic heat transport (PW) in pre-PRIMAVERA models.

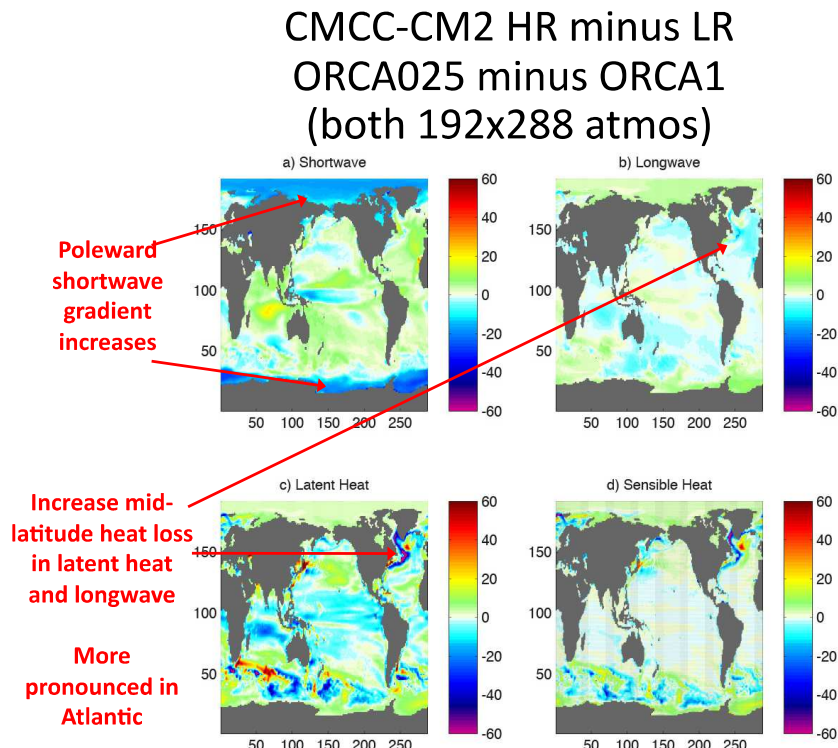


Figure 2: Difference in mean surface flux components (Wm^{-2}) in the pre-PRIMAVERA high and low resolution versions of CMCC-CM2.

3.1.2. Deep water convection (SMHI)

We analyzed the effect of high resolution on the deep water formation using standard (~1°) and high-resolution (~0.25°) simulations from five different coupled Global Climate Models (GCMS) (Table 1). To analyze the strength of the deep water formation, we used a convection index, which only takes the mixed water masses in the convection regions below a specific depth into account, the deep mixed volume (DMV; Brodeau and Koenigk, 2016).

The mixed layer depth shows strong variations across models, particularly in the Labrador Sea (Fig. 3). Here, a few models show deep convection down to the bottom of the ocean every year, while others do not show any deep mixing. Compared to observations from ARGO-floats (Holte et al., 2010), most of the models overestimate the deep water formation, particularly in the Labrador Sea. The averaged DMV over all high-resolution models show increased deep convection in the Labrador Sea but decreased convection in the Greenland-Iceland-Norwegian (GIN) Seas compared to the average over the standard resolution model simulations (Table 2). However, this response is not robust across all models. Further, we find from the CMCC-simulations, that the convection is weaker in the pre-industrial simulations compared to the present day simulations. The HadGEM-model ensemble indicates decreased convection in the Labrador Sea with increasing atmospheric resolution.

The convection in the Labrador Sea is largely governed by the ocean heat release to the atmosphere in the convection area. Northwesterly atmospheric flows, which are often connected to a positive state of the North Atlantic Oscillation (NAO), increase the ocean heat release and thus the density of the ocean surface. We found that the high-resolution models show stronger surface heat fluxes than the standard resolution models in the convection areas. This agrees with the stronger convection in the Labrador Sea in the high-resolution models. Also in the GIN Seas, high resolution leads to increased ocean heat release to the atmosphere. However, the relation between surface heat fluxes and convection is strongly model dependent.

Model	Ocean Resolution	Atmos Resolution	Simulations
EC-Earth3.1	ORCA1 - 1°	T255	1950-2009 (historical)
	ORCA025 - 1/4°	T511	1990-2014 (historical)
MPI-ESM	TP04 – 0.4°	T63	55-year PI
	TP6M – 1/10°	T63	55-year PI
CMCC-CM2	ORCA1 - 1°	~0.8°x1.1°	40-y PI, 300-y PD
	ORCA025 – 1/4°	~0.8°x1.1°	40-y PI, 40-y PD
CERFACS-HR	ORCA025 – 1/4°	T359	50-year PD
HadGEM-GC2	ORCA025 – 1/4°	N96, 216, 512	3 x 100-year PD

Table 1: Model versions and simulations.

Metric for deep water formation and surface heat flux	Model-mean Standard resolution	Model mean High resolution
Labrador Sea, DMV-metric, zcrit=0m	0.83	1.13
Labrador Sea, DMV-metric zcrit=1000m	7.6	10.3
Labrador Sea, Surface heat flux-metric	0.97	1.23
GIN Sea, DMV-metric, zcrit=0m	1.24	0.8
GIN Sea, DMV-metric, zcrit=700	4.08	1.54
GIN Sea, Surface heat flux-metric	0.99	1.13

Table 2: Comparison of deep mixed volume (DMV) and surface heat fluxes (SHF), averaged over all standard and high-resolution models, and in observations in the Labrador Sea and the GIN-Sea. The DMV-metric is defined as the quotient of the model DMV and the observed DMV from ARGO-floats. The SHF metric is defined as the quotient of the model surface heat flux and the observed heat flux in the respective box. Values larger (smaller) than 1 show an overestimation (underestimation) of the models.

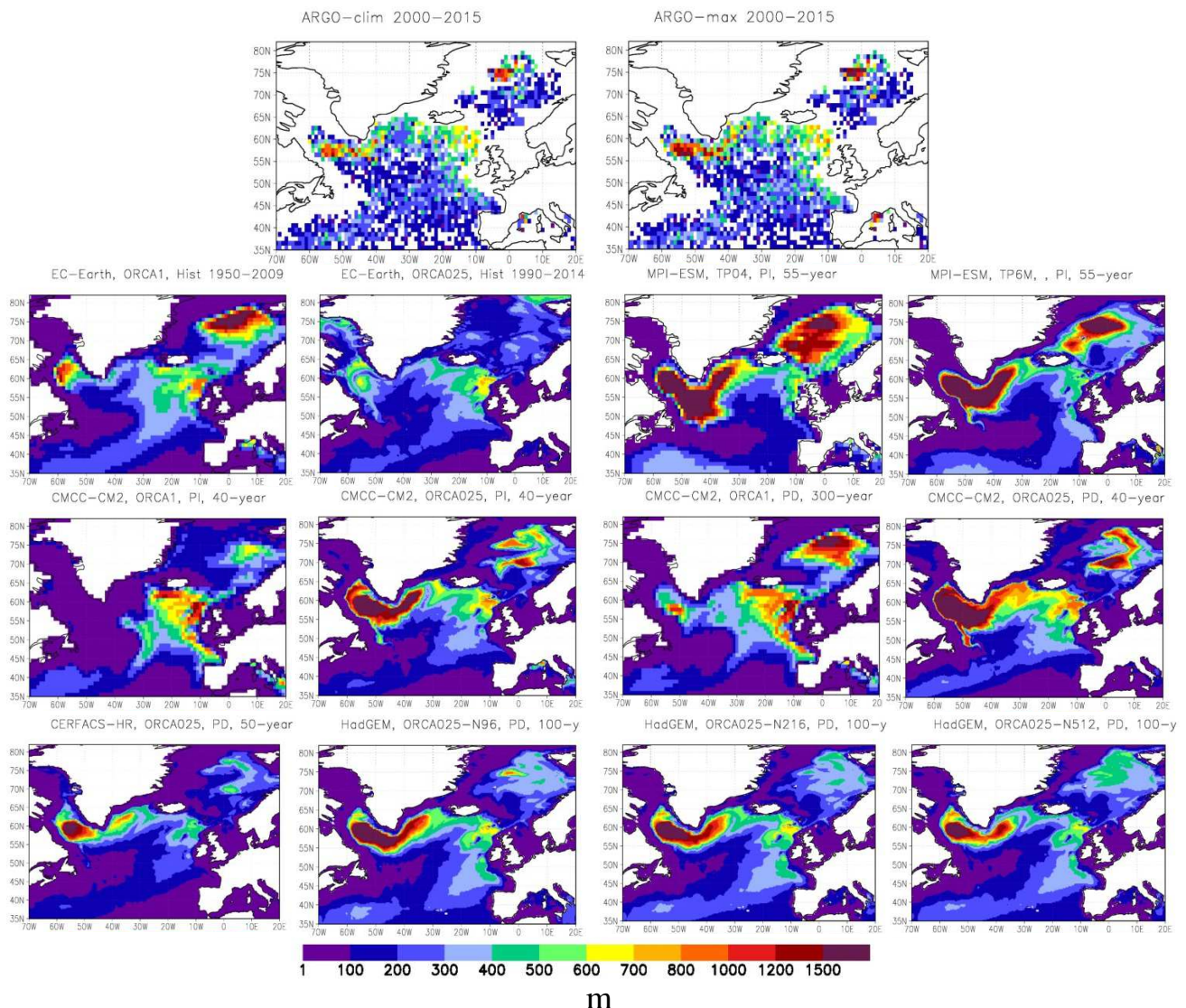


Figure 3: Mixed layer depth in March, averaged over the entire length of the model simulations. Top row: Climatology over years 2000-2015 and maximum values from ARGO-floats (observations). Rows 2-4: Model simulations.

3.1.3. Gulf Stream current in coupled models (CERFACS)

The 15°C isotherm depth at 200 m depth has been used as a simple metric to characterise the Gulf Stream pathway through the pre-PRIMAVERA runs. 10 model (atmosphere and ocean) resolutions have been compared, together with 4 reference products (ORAS4, ORAP5, WOA13, GLORYS). Fig. 4 shows that the Gulf Stream pathway differs in the different reference datasets (observations and reanalysis) used, indicating the utility of using different observational products when evaluating climate models. There is not a clear link between the model resolution and the representation of the Gulf Stream pathway, in particular when comparing ORCA1 (o1) and ORCA025 (o25) type resolutions. It is clear there is improvement for the ORCA12 NEMO (meto_o12). The weak difference between o1 and o25 could depend on sea surface temperature (SST) biases in individual models, and also on the atmospheric resolution. This could also indicate that the 15° isotherm at 200m is not a good metric to explore the Gulf Stream pathway representation. Other metrics will be explored and designed in the following months.

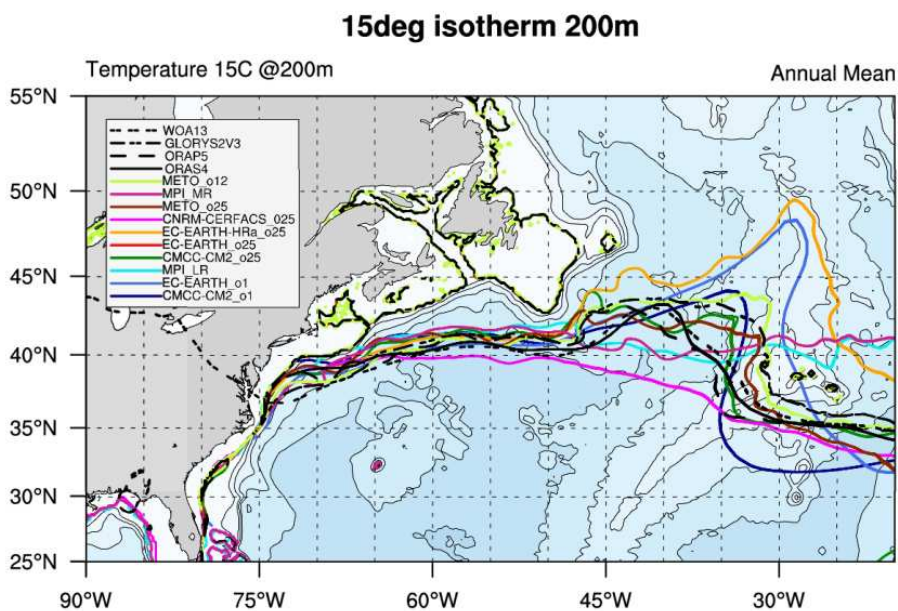


Figure 4:

15°C isotherm depth at 200 m depth for 10 different pre-PRIMAVERA runs considering different ocean and atmosphere model resolution (colors). Black lines represent different reference datasets (ORAS4, ORAP5, GLORYS, WOA13).

3.1.4. Gulf Stream jet variability (NMA / SMHI)

We analyzed the impact of changing resolution in a coupled model, on the Gulf Stream jet and its variability. The analysis will then be replicated on an ensemble of coupled models in order to assess the robustness of the results. The aim is to improve the Gulf Stream model representation and to understand and represent its links to the Northern Hemisphere (focus on Europe) climate.

The model used here is EC-Earth, run by SMHI in two configurations: T511 (atmosphere) with 0.25° (75 levels) in the ocean (HR - high resolution), and T255 (atmosphere) with 1° (75 levels) in the ocean (LR - low resolution). The two runs (HR and LR) have the same external forcing and the same starting date. We used observations from Aviso/Cnes and ERA-Interim. We compared the two runs (HR and LR) over a common period of 20 years: 1990-2009 and performed a grid-point, spectral and teleconnections analysis.

Here are the main results of this analysis:

- Climatological features of the mean Gulf Stream are better captured in the HR configuration. The main differences appear in a stronger sea surface temperature (SST) gradient of the Gulf Stream and increased rotational kinetic energy (wavy jet), both in agreement with observations. These are further driving differences in the position of the main deflection points and in the latitude of the jet.
- We used spectral decomposition of de-trended SST time series and compared variance for HR and LR at the same locations (Fig. 5). We note that in all locations (except Labrador, point 5 - where ice-interaction processes are important), lower resolution is associated to a spectral shift towards lower frequencies. This aspect, if robust, could be of high relevance for multi-year (and possibly seasonal) prediction.
- We compared Gulf Stream remote links in HR and LR in two aspects:
 - 1) South latitudes Gulf Stream driving GSE variability and its feedback: The analysis of HR and LR indicates that the jet slope in the downstream of the Grand Bank (GB) deflection (points 2-6 in Fig. 5) appears to play an important role in the link between Gulf Stream and its Northward extension GSE. This slope is positive in LR (a reduced GB deflection), allowing warm advection and flow split at Eastern longitudes, or an E-NE main track of GSE, in opposite to a N-NE track under an earlier and stronger GB diffluence in HR. This creates low contribution from thermal advection to vorticity in the LR case. Opposite response is obtained for HR, where positive vorticity damps anticyclonic re-circulation and allows a Northward mean track (Fig. 5, right panel). Hence, lower latitude jet enhances (the opposite for higher latitudes) the GSE heat transport along its main axes (A1, A2, A3 in Fig. 5) in HR while damping it in LR.
 - 2) GSE co-variability (inter-correlations of axes north-edges: A1, A2 and A3) remain unchanged in LR and HR. Also the Labrador-West UK (point 5 - A1 in Fig. 5) lagged link (of period $T \sim 6a$ in HR) remains significant but has a main period of only $T \sim 2a$ in LR case.

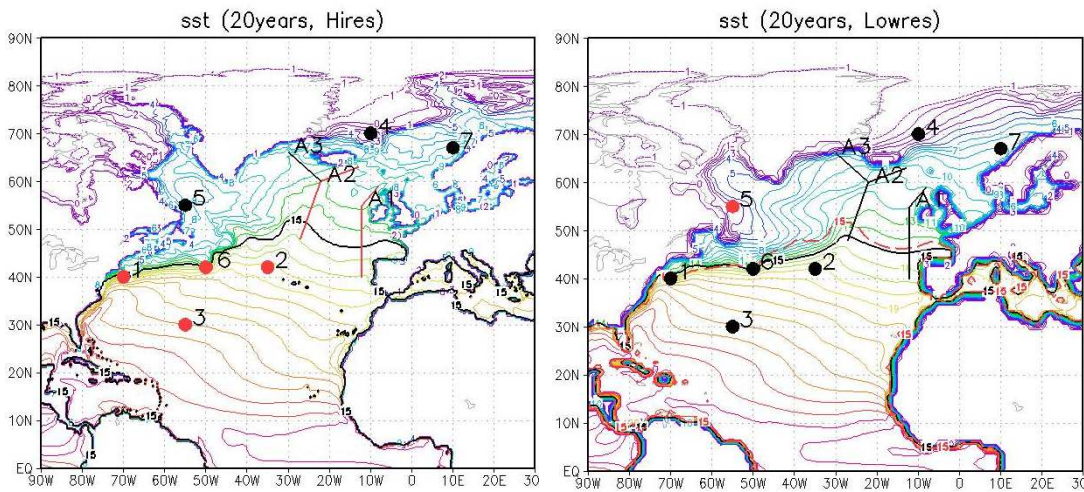


Figure 5: Sea surface temperature (SST) (mean 1990-2009) for EC-Earth at high resolution (left) and low resolution (right). Isotherm 15°C is the black thick line in the left panel and the dashed red line in the right panel. Red bullets and axis indicate high frequency of the main variability (~5a); black bullets and axis indicate low frequency of the main variability (~10a).

3.1.5. Ocean heat content changes (BSC)

We analyzed the impact of model resolution on ocean heat content trends and SST trends. We used two experiments with present day forcing (of year 2000) and 100-years long of the Met Office Hadley Centre Global Environment Model version 3 HadGEM3-GC2. Both experiments include the NEMO ocean model and CICE sea ice model at ORCA025 resolution ($\sim 1/4^\circ$); one experiment is coupled to the atmosphere UM model at N96 resolution ($\sim 130\text{km}$) and the second one to the atmosphere UM model at N512 resolution ($\sim 25\text{km}$).

We find that the SST patterns in decades with positive SST trends are anti-symmetrical to the ones in decades with negative SST trends (Fig. 6). On positive (negative) SST-trend decades there is a warming (cooling) in the tropical Pacific, in the subpolar gyre in North Atlantic and in the Ross Sea in the Southern Ocean. The patterns are very similar between the two different resolutions, with exceptions in the high latitudes and the subtropical Atlantic gyre where N512O025 has stronger SST trends than N96O025.

The total ocean heat content trends show that major changes take place in the Atlantic and Southern Oceans (Fig. 7). In decades with positive SST trends there is heat content increase in the Atlantic and Southern Oceans, while there is heat content decrease in the Pacific. In decades with negative SST trends, the pattern is the opposite.

We plan to extend this analysis to other models of the pre-PRIMAVERA and PRIMAVERA database, and forced standalone ocean models in order to address the relationship between SST trends and ocean heat content changes at different depths and the impact of atmospheric resolution.

SST trends (degK/decade)

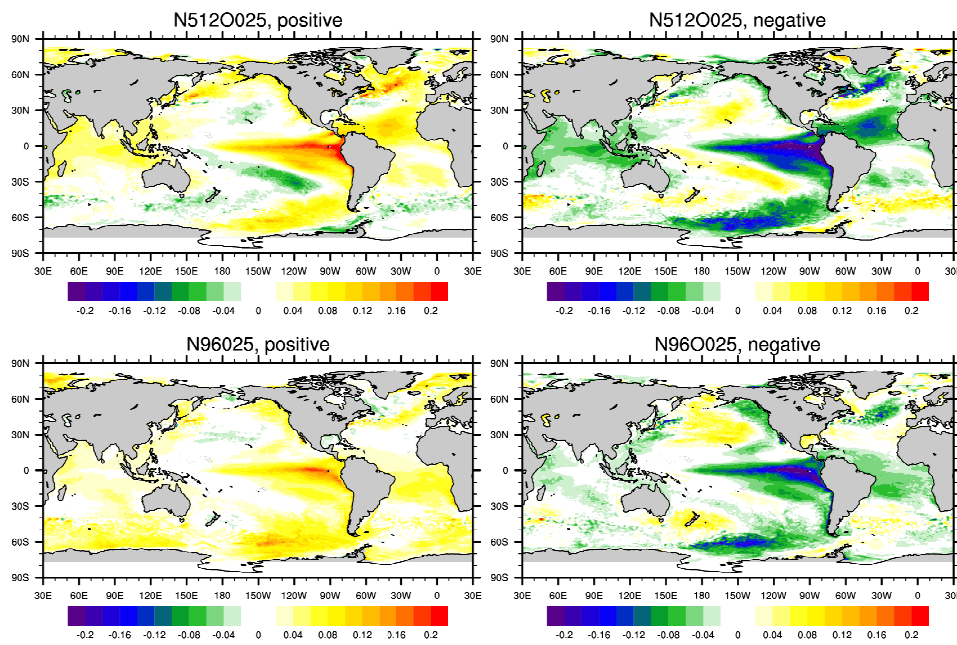


Figure 6: SST trends (degK/decade) for decades with positive SST trends (left) and negative SST trends (right). Top and bottom panels show results from the high and low atmosphere resolution experiments, respectively. The trends are calculated with linear regression from annual mean SST data.

OHC trends (W/m²)

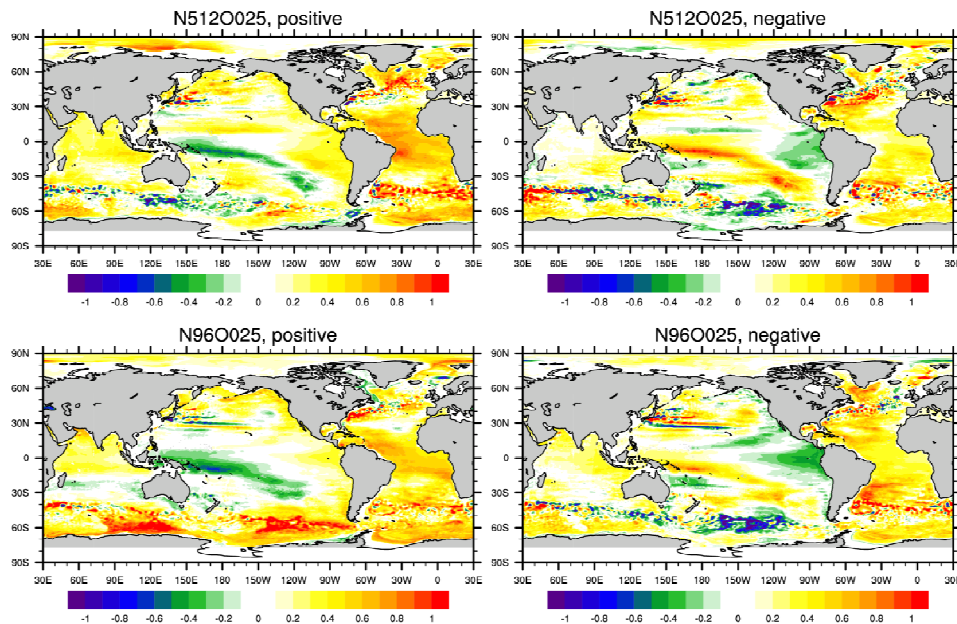


Figure 7: Ocean heat content trends (W/m²) for decades with positive SST trends (left) and negative SST trends (right). Top and bottom panels show results from the high and low atmosphere resolution experiments, respectively. The trends are calculated with linear regression from annual mean OHC data.

3.1.6. Air-sea coupling (MET OFFICE)

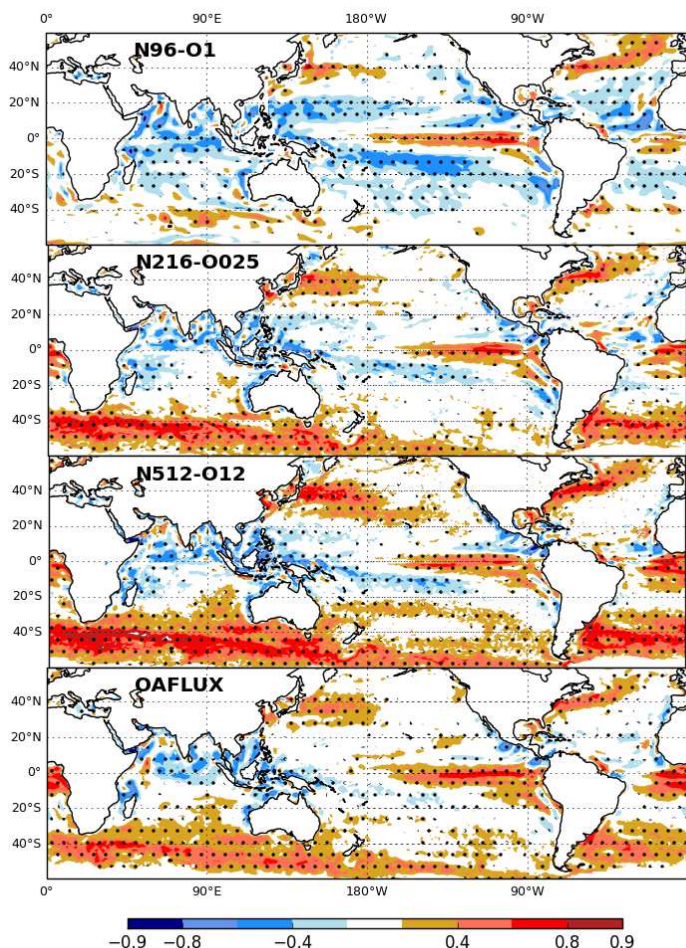
The strength of coupling and exchanges of heat and moisture between atmosphere and ocean are key processes in climate. They are also very difficult to observe since the most energetic exchanges occur in ocean boundary current regions (such as the Gulf Stream), where the exchanges also lead to cloud cover and hence make remote sensing difficult. Analysis of climate models with ocean resolution approaching 10km can offer some insight into these processes.

Parallel coupled climate simulations with ocean resolutions of $1/4^\circ$ and $1/12^\circ$ have been completed at the Met Office as preparation for the PRIMAVERA Stream 1 and WP4 simulations. These are documented in Hewitt et al. (2016), and analysis (partly funded by PRIMAVERA) is in Roberts et al. (2016). Further analysis has now included an ocean model with 1° resolution, which is more typical of CMIP-type models.

One of the key metrics found to assess coupling is the temporal co-variability of sea surface temperature (SST) and surface wind stress. The methodology is described in Roberts et al. (2016), and essentially looks at the correlation of monthly means (of daily spatially-filtered anomalies) of SST and wind stress.

Observations show regions where the SST and wind stress are strongly correlated (Fig. 8), typically near to high SST gradient regions, and these are interpreted as regions where the ocean is driving the atmospheric variability. Both the $1/4^\circ$ and $1/12^\circ$ models seem to capture the observed pattern well, while the 1° model is much poorer, particularly in the Southern Ocean and with stronger negative correlations elsewhere. A multi-model analysis using Stream 1 simulations will help to understand how robust and how important such differences are, and their implications for European climate.

Figure 8: The correlation of SST and wind stress from HadGEM3-GC2.1 model. From top to bottom: N96-O1 is 130km- 1° ; N216-O025 is 60km- $1/4^\circ$; N512-O12 is 25km- $1/12^\circ$; and observations are from OAFLUX.





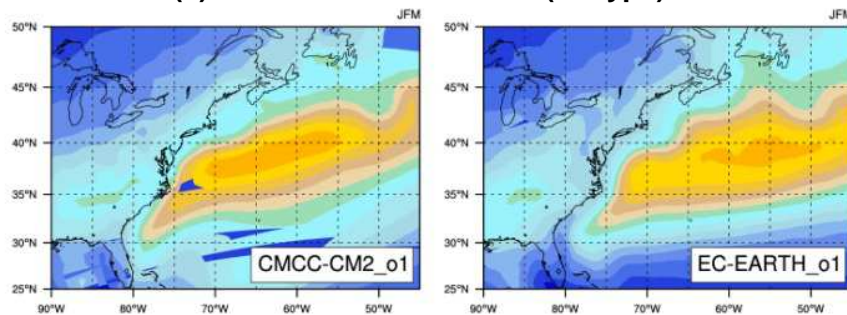
3.1.7. Air-sea interactions in the Gulf Stream region (CERFACS)

We have studied the spatial pattern of winter (DJF) turbulent heat fluxes (latent + sensible) in the different pre-PRIMAVERA runs. Pre-PRIMAVERA runs have been divided into 3 groups according to the resolution of the ocean model: low resolution (o1 type), medium resolution (o25 type) and high resolution (o12 type). We have examined the magnitude and the spatial pattern of the heat flux. Results (not shown here) suggest that low and medium resolution models lead to stronger values of the fluxes in general. Finest scale structures are clearly evident in the higher resolution model (o12) with stronger values near the coast and decreasing off shore. However, low-resolution models (cmcc_o1) show a spatial structure and values for the turbulent heat fluxes very similar to the medium-resolution model. For low and medium resolution models there is not a clear difference in the simulated heat fluxes. More investigation is needed (role of the SST, atmospheric biases etc).

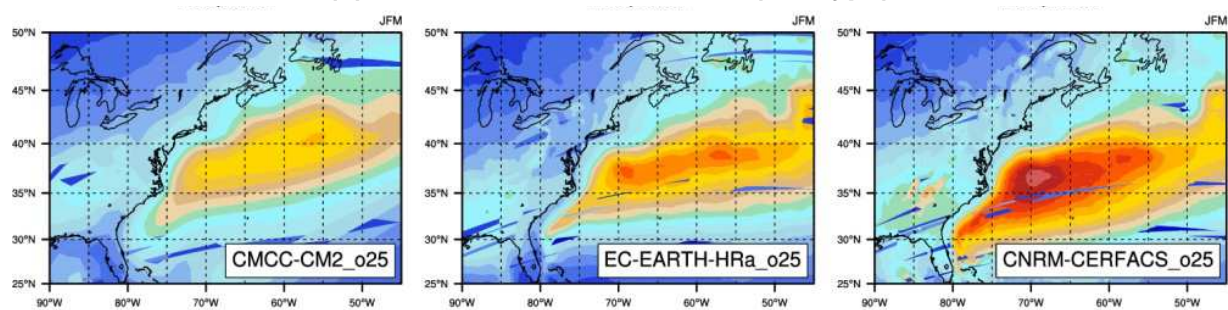
3.1.8. Impact of SST gradients and mesoscale activity on the marine boundary layer (CERFACS)

We have analyzed the magnitude and the spatial pattern of the winter (DJF) precipitation for the 3 groups of models according to the previous section. Fig. 9 clearly shows that the very high-resolution model (012) is the best model in representing the precipitation structure from the satellite observations (also shown in Minobe et al., 2008). The low-resolution models (o1 type) are not able to represent the fine scale structure and the observed precipitation field. However, the improvement of medium resolution models is not clear: o25 group of models does not lead necessarily to a better representation of the winter precipitation field.

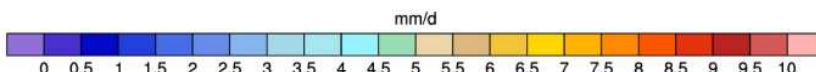
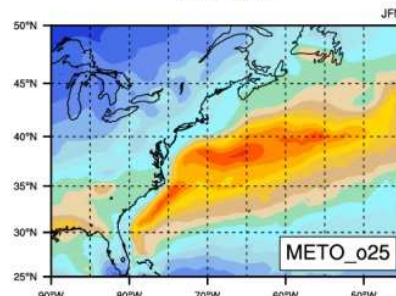
(a) Low resolution models (o1 type)



(b) Medium resolution models (o25 type)



Precipitation



(c) High resolution model (o12 type)

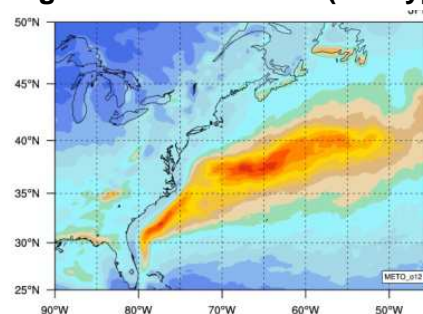


Figure 9: Precipitation from different pre-PRIMAVERA models.

3.1.9. AMOC lead and lag correlation (CNR)

The impact of resolution on Atlantic Meridional Overturning Circulation (AMOC/AMO) lead and lag correlation was analyzed based on pre-PRIMAVERA outputs with ESMValTool. Due to the length of the experiments, we only used HadGEM3-GC2 (N96O-025 and N216-O025) from MetOffice. The difference between HadGEM3-GC2 N96-O025 and N216-O025 is only from the atmospheric model resolution (the former is 135 km, while the latter is 60 km).

The analysis is based on 61 years of data out of the 100 years available. The AMOC/AMO lead and lag correlation is calculated based on the first PC annual mean time series of AMOC and AMO annual mean time series. In general the AMOC/AMO lead and lag correlation in N216-O025 and N96-O025 (Fig. 10) is very similar. In N216-O025, the AMOC leads AMO around 1 year and in N96-O025 the AMOC leads AMO around 2 years. The reason why the lead and lag correlation is around 1/2 year could be because of the strong positive anomaly (Fig. 11) in the beginning of the record for both AMOC and AMO, which, since the record is relatively short, could affect this estimate. As soon as longer time record is available (these experiments are 100 year long, but so far only the first 60 years have been post-processed for this analysis), a more refined analysis needs to be done in order to verify how sensitive is the lead and lag correlation to the record length. The AMOC meridional streamfunction climatology over the 61 years in N96-O025 and N216-O025 is almost identical (not shown here) indicating that the impact of atmospheric resolution on AMOC and the lead and lag correlation between AMOC/AMO is negligible (Fig. 10).

As a next step, we would like to extend the work to the impact of ocean model resolution on the AMOC/AMO lead and lag correlation with PRIMAVERA outputs, especially with long time integrations.

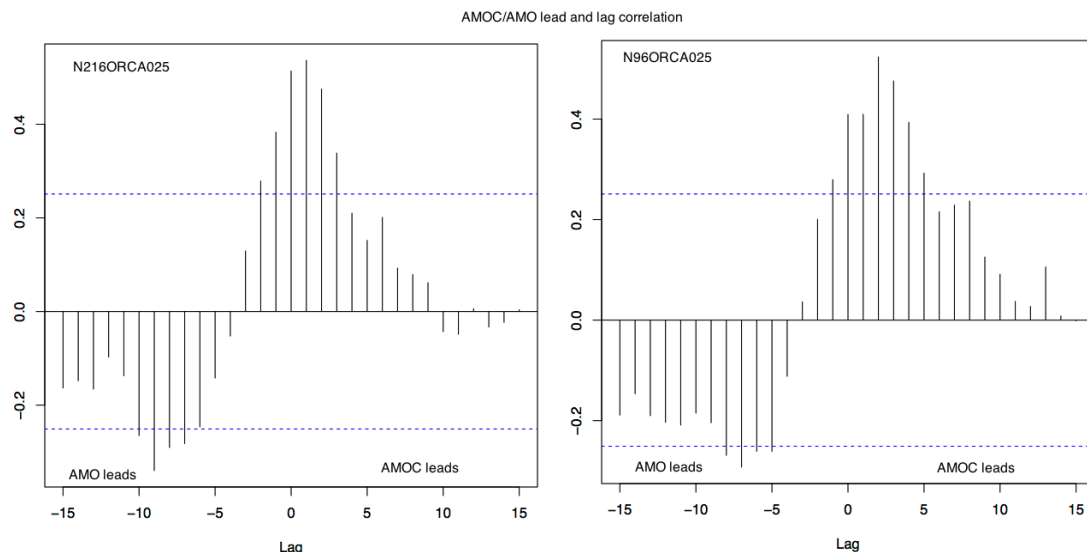


Figure 10: AMOC PC1 and AMO lead and lag correlation in MetOffice HadGEM2-GC2 model (left: N216-O025, right: N96-O025).

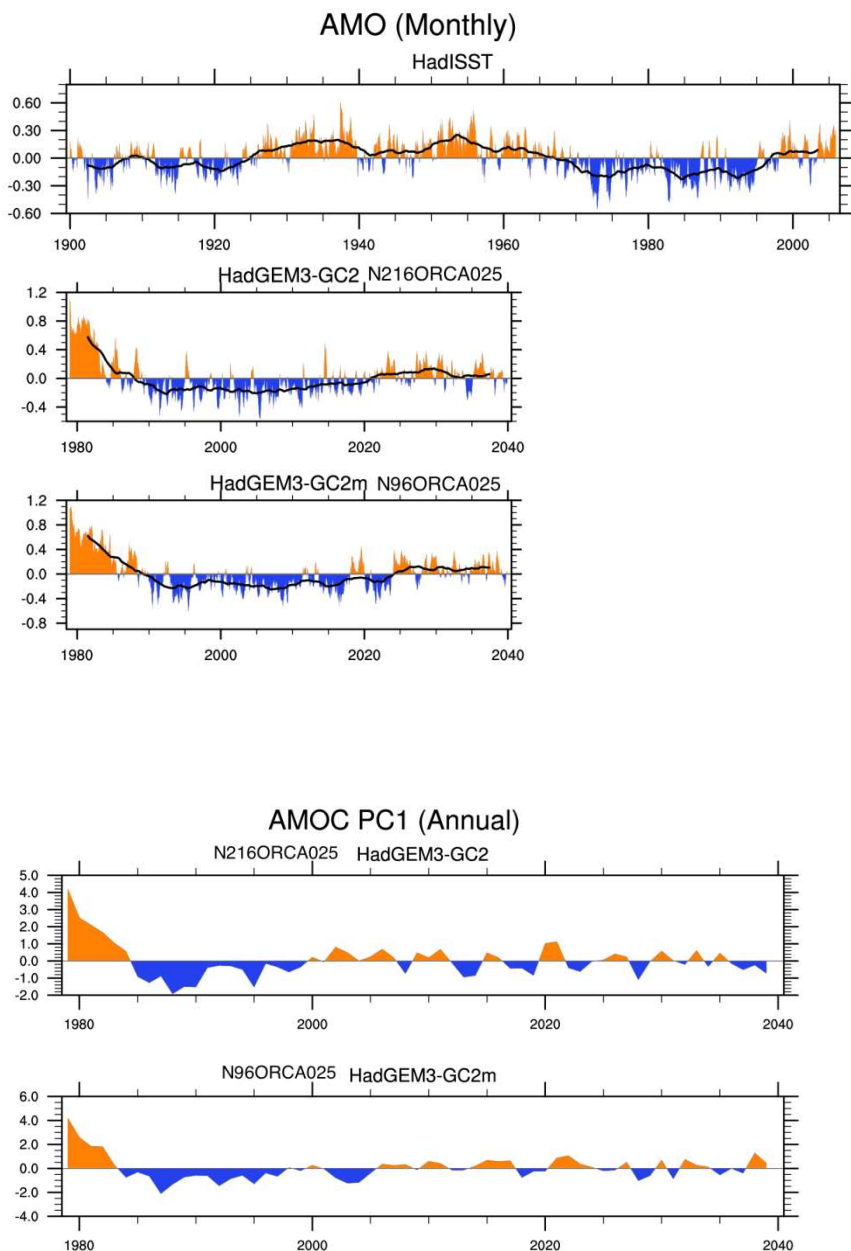


Figure 11: Top panels: Time series of the AMO in HadISST and HadGEM3-GC2 (N216-O025 and N96-O025). Bottom panels: Time series of the AMOC PC1 in HadGEM3-GC2 (N216-O025 and N96-O025).

3.1.10. Tropical Atlantic SST bias (MPG)

MPI-ESM simulations applying a horizontal grid configuration with relatively low resolution (atmosphere 1.8°, ocean 0.4°) show a warm bias of several degrees in the tropical Atlantic SST along the African coast (Fig. 12a). Milinski et al. (2016) have investigated the impact of increased atmospheric and oceanic resolution on the SST bias. A simulation with increased oceanic (0.1°) but unchanged atmospheric resolution shows a similar SST bias as the original simulation (Fig. 12c). Increased atmospheric resolution (0.5°), on the other hand, strongly reduces the SST bias, independent of the oceanic resolution (Fig. 12b and 12d). The improvements are due to a better representation of the low-level wind jet which affects the upwelling in the ocean. Sensitivity experiments suggest that about half of the reduction in the SST bias can be attributed to a better resolved coastal orography that affects the representation of the wind jet.

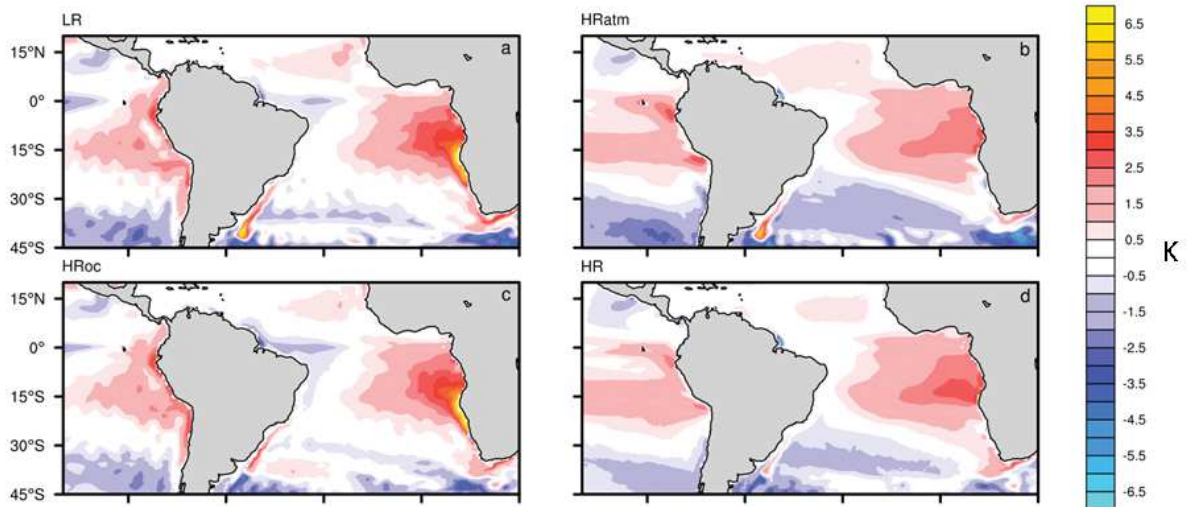


Figure 12: Tropical Atlantic SST bias in MPI-ESM with different horizontal resolutions: (a) atmosphere 1.8°, ocean 0.4°, (b) atmosphere 0.5°, ocean 0.4°, (c) atmosphere 1.8°, ocean 0.1° and (d) atmosphere 0.5°, ocean 0.1°.

3.1.11. Vertical heat and salt fluxes (MPG)

The eddy heat and salt fluxes simulated by the 0.1 degree MPIOM ocean model transport heat and salt upward, counteracting the respective fluxes due to the time-mean circulation. The related tendency forcing acts to cool and freshen water masses at the intermediate depths, reducing the long-standing model biases there. This resolved eddy effect cannot be completely represented using the standard eddy parameterizations, mainly because the net effect of these parameterizations depends not only on the parameterized eddy-induced velocities, but also on the tracer gradients and the isoneutral slopes simulated by the low-resolution model. The latter can render the net parameterized tendency forcing such that using eddy parameterizations further worsens the model performance. The result suggests that we cannot really rely on parameterizations of unresolved eddies. Resolving eddies is

Key findings for North Atlantic Ocean:**a) *Results including multiple models:***

- Atlantic Ocean heat transport is increased when there is an increase in ocean resolution from 1° to $1/4^{\circ}$, more in line with observations, while there is no significant change by increasing atmospheric resolution alone (**NERC**).
- High resolution strengthens deep convection in the Labrador Sea and reduces deep convection in the GIN Seas (**SMHI**).
- There is not a clear link between the model resolution and the representation of the Gulf Stream pathway, in particular when comparing 1° and $1/4^{\circ}$ ocean resolutions. However, it is clear there is an improvement when using NEMO-1/ 12° (**CERFACS**).
- For low and medium resolution models there is not a clear difference in the simulated heat fluxes. Finest scale structures are clearly evident in the higher resolution model ($1/12^{\circ}$) with stronger values near the coast and decreasing off shore (**CERFACS**).
- The very high-resolution model ($1/12^{\circ}$) is the best model in representing the precipitation structure from the satellite observations. The low-resolution models (1°) are not able to represent the fine scale structure and the observed precipitation field. However, the improvement of medium resolution models ($1/4^{\circ}$) is not evident (**CERFACS**).

b) *Results including only one model (at different resolutions):*

- Increased resolution with EC-Earth has a positive impact on the key Gulf Stream jet variability, and this further improves both local processes and remote North Atlantic teleconnections (**NMA/SMHI**).
- SST trend patterns are very similar between two HadGEM3-GC2 model simulations using different atmosphere resolutions, with exceptions in the high latitudes and the subtropical Atlantic gyre where the higher resolution simulation N512O025 has stronger SST trends than N96O025 (**BSC**).
- Both $1/4^{\circ}$ and $1/12^{\circ}$ resolutions with HadGEM3-GC2.1 model seem to capture the observed pattern of correlation between wind and SST well, while the 1° model is much poorer, particularly in the Southern Ocean and with stronger negative correlations elsewhere (**MET OFFICE**).
- The AMOC/AMO lead and lag correlations in HadGEM3-GC2 with two different atmosphere resolutions (60 and 135 km) are very similar (**CNR**).
- The warm bias of several degrees in the tropical Atlantic SST along the African coast in MPI-ESM is strongly reduced with increasing atmospheric resolution due to a better representation of the low-level wind jet which affects the upwelling in the ocean (**MPG**).

3.2. Arctic sea ice

3.2.1. Heat conduction index (UCL / BSC)

The heat conduction index is a novel diagnostic that characterizes and quantifies the process of vertical heat conduction through the sea ice-snow medium during growth season. It was formally defined as the sensitivity of *internal* system temperature (taken at the ice-snow interface) to the *surface* temperature (taken at the atmosphere-snow interface). When a simple snow + ice configuration is assumed with one layer each and constant heat conductivities, this heat conduction index (HCI) can be expressed as:

$$HCI = \frac{k_s h_i}{k_i h_s + k_s h_i}$$

where h denotes thickness, k heat conductivity and the subscripts i and s stand for ice and snow, respectively. The heat conduction index was diagnosed from two stand-alone integrations of the ocean-sea ice model NEMO-LIM3.6 forced by identical atmospheric forcing (Fig. 13). A notable aspect of this diagnostic is that it is rather insensitive to the increase in resolution. That is, the way that internal system thermodynamics responds to the external forcing is rather independent of the horizontal resolution – although the mean states are readily different as suggested by the sea ice thickness maps.

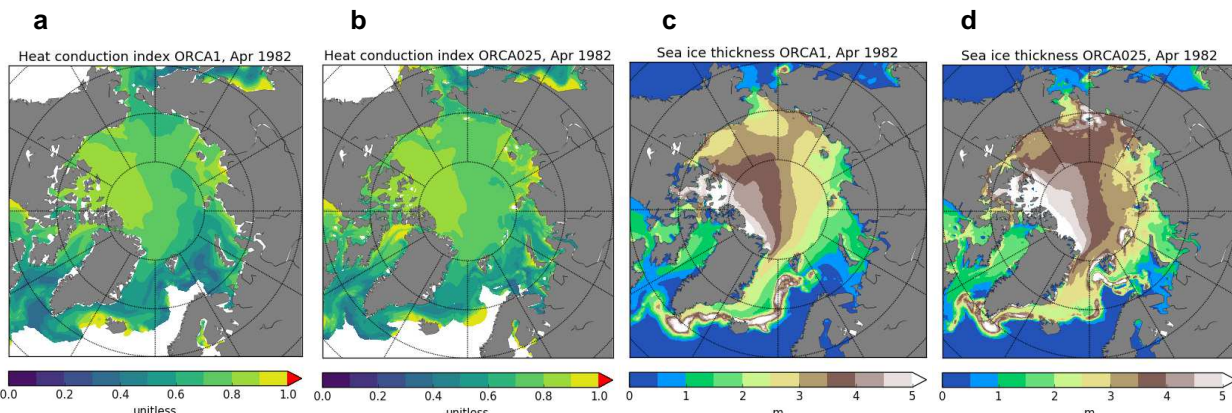


Figure 13: Left panels (a, b): Sea ice heat conduction index diagnostic applied to two NEMO-LIM3.6 simulations, at (a) standard ($\sim 1^\circ$, left) and (b) high ($\sim 0.25^\circ$, right) resolutions for April 1982 in a stand-alone ocean-sea ice simulation. Right panels (c, d): Sea ice thickness at (c) standard and (d) high resolutions.

3.2.2. Sea ice drift-strength feedback (UCL)

The sea ice drift-strength feedback diagnostic is a scatter plot that relates sea ice drift speed to sea ice concentration and thickness, averaged over a period that is large enough (typically 20 to 30 years) and over the Central Arctic. Sea ice drift speed is normalized by wind friction speed in order to take away the role of wind (Olason and Notz, 2014). According to observations, sea ice drift speed increases with decreasing concentration and thickness, with a hysteresis behavior for thickness (Olason and Notz, 2014). This analysis has been applied to NEMO-LIM3.6 ocean-sea ice model (forced by atmospheric reanalysis) at two different resolutions (1° and 0.25°). Results show that the model captures the relationships

between drift speed, concentration and thickness compared to observations, which does not seem to be obvious as some other models do not capture those relationships (Fig. 14). The higher resolution does not significantly change the results in terms of sea ice drift speed and concentration. However, mean sea ice thickness increases by about 30 cm when running the model at high resolution (Fig. 14). The higher thickness with higher resolution seems to be caused by a negative thermodynamic feedback between sea ice thickness distribution and heat loss to the atmosphere (Massonet et al., in prep.; see diagnostic below). An article focusing on this diagnostic with NEMO-LIM3.6 is in preparation (Docquier et al., in prep.) and Python scripts to compute it are available on JASMIN. There are three drawbacks to this analysis: 1) sea ice drift is computed from monthly components of sea ice velocity as daily values are not available in pre-PRIMAVERA model outputs other than NEMO-LIM3.6; 2) only three pre-PRIMAVERA runs could be analyzed using this diagnostic due to the lack of sea ice outputs during the period 1958-1980 for other models; 3) the version of NEMO-LIM used in EC-Earth3.1 is an older version (NEMO3.3.1-LIM3).

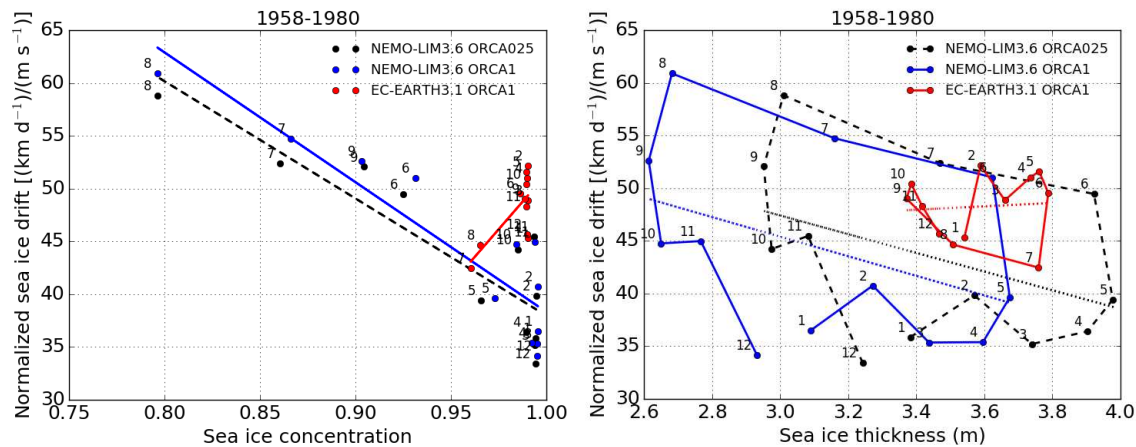


Figure 14: Multi-year monthly mean normalized sea ice drift speed against (a) sea ice concentration and (b) sea ice thickness, averaged over 1958-1980 and over the Central Arctic, for three different model simulations (NEMO-LIM3.6 forced by DFS5.2 with ORCA025 and ORCA1 and EC-Earth3.1 with ORCA1). Each dot represents a month of the year.

3.2.3. Sea ice thickness variance (UCL / BSC)

A diagnostic was developed to understand the increased sea ice thickness at higher horizontal resolution (Fig. 13c and 13d). A theoretical framework was derived to link the vertical heat conduction flux Q to the mean sea ice thickness in a control region μ and the sea ice thickness standard deviation σ in that region. It can be proven that the vertical heat conduction flux, and as a consequence basal ice growth rates, increases as the variance of sea ice thickness (Massonet et al., in prep.). That is, for the same average sea ice thickness over a given domain, highly heterogeneously distributed sea ice will grow faster than ice of uniform thickness over that domain. A diagnostic of variance in sea ice thickness was created based on the information available from LIM3: this model keeps track of the sub-grid scale information on sea ice thickness (Fig. 15). The increased variance in sea ice thickness in the high resolution integration confirmed the conceptual argument explained above.

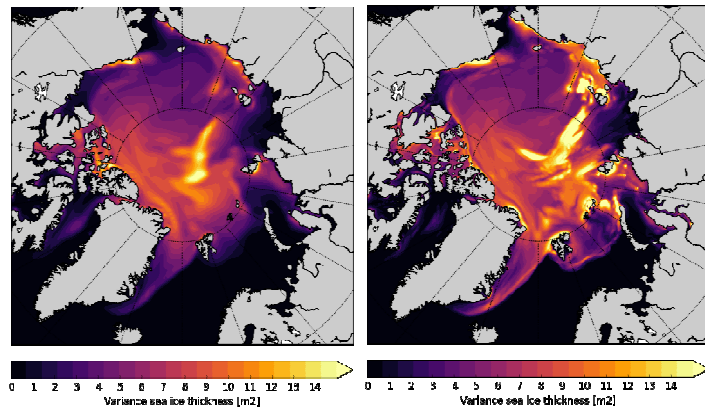


Figure 15: Sub-grid scale variance of sea ice thickness in the sea ice model LIM3 in the same two integrations as in Fig. 13, for the month of January 1961, that is, 3 years after the start of both simulations from a common initial sea ice thickness state. Left: ORCA1; right: ORCA025.

3.2.4. Sea ice areas (SMHI)

The sea ice areas and variations for 8 different Arctic regions have been calculated for all models in Table 1 and compared to satellite ice products of OSISAF (Eastwood et al., 2011) and OISSTv2 (Reynolds et al., 2002). The average of the standard resolution models overestimates the ice area in all regions except for the Central Arctic in September (20-40% depending on the reference data set for the entire September Arctic ice area). The average of the high resolution model simulations show a somewhat smaller and more realistic ice area in September and the entire Arctic ice area compares well to the satellite data sets (Table 3). In March, both standard and high resolution models simulate realistic ice areas, indicating that the annual cycle is better represented in the high resolution models.

Comp OISSTv2/ OSISAF	NH	Labrador Sea/ Baffin Bay	Greenland Sea	Barents/ Kara Seas	Laptev/ East Sib Seas	Chukchi/ Bering Seas	Beaufort Sea	Central Arctic
SR Model	1.41	9.23	2.56	3.44	2.11	1.54	1.33	0.98
mean	1.24	3.40	1.87	2.31	1.79	1.27	1.15	0.92
HR Model	1.11	3.04	1.02	1.67	1.35	1.33	1.29	0.90
mean	0.97	1.12	0.75	1.12	1.15	1.09	1.12	0.85

Table 3: Quotient of simulated ice area in Arctic regions and ice area derived from OISSTv2 and OSISAF (*italic*) satellite products. Values larger (smaller) than 1 show an overestimation (underestimation) of the models.

3.2.5. Atmospheric response to sea ice variability (SMHI)

We investigated the atmospheric response to sea ice variability in the eight Arctic regions mentioned in section 3.2.4. Koenigk et al. (2016) found that sea ice in November over the entire Northern Hemisphere (NH), and particularly over the Central Arctic (CARC), and the Barents/Kara (BAKA) Seas seem to be important for the sign of the following winter North Atlantic Oscillation (NAO); particularly they found a pronounced negative NAO in the winter after a November with low sea ice concentration in the BAKA-region. Here, we analyze if the Earth System Models participating in the PRIMAVERA Project (Table 1) reproduce the PRIMAVERA (641727) Deliverable D2.1

observed features, focusing particularly on the impact of ocean resolution on the linkage between sea ice and atmospheric circulation. Our analysis is performed dividing the models depending on their ocean resolution, grouping in two main groups: high (0.25°) resolution and low (1°) resolution.

Most of the high ocean resolution GCMs reproduce the observed spatial pattern and sign of correlation between November concentration in NH, CARC and BAKA regions and winter sea level pressure (Fig. 16a, 16c, 16e). As for observations, this would imply that the models show that a decrease of concentration over the mentioned regions might be promoting a negative phase of the NAO. However, the correlation coefficients are much smaller in the models compared to the observations.

In contrast, most of the low ocean resolution GCMs show the opposite correlation pattern compared to observations (Fig. 16b, 16d, 16f). Even here, correlation values are generally rather small. Still our results indicate that the ocean resolution, and possibly the improved representation of particularly summer sea ice, might be an important factor in capturing processes related to sea ice concentration and their relationship with the atmospheric circulation. Further analysis is needed to understand the possible causes for the improvement in the high resolution simulations.

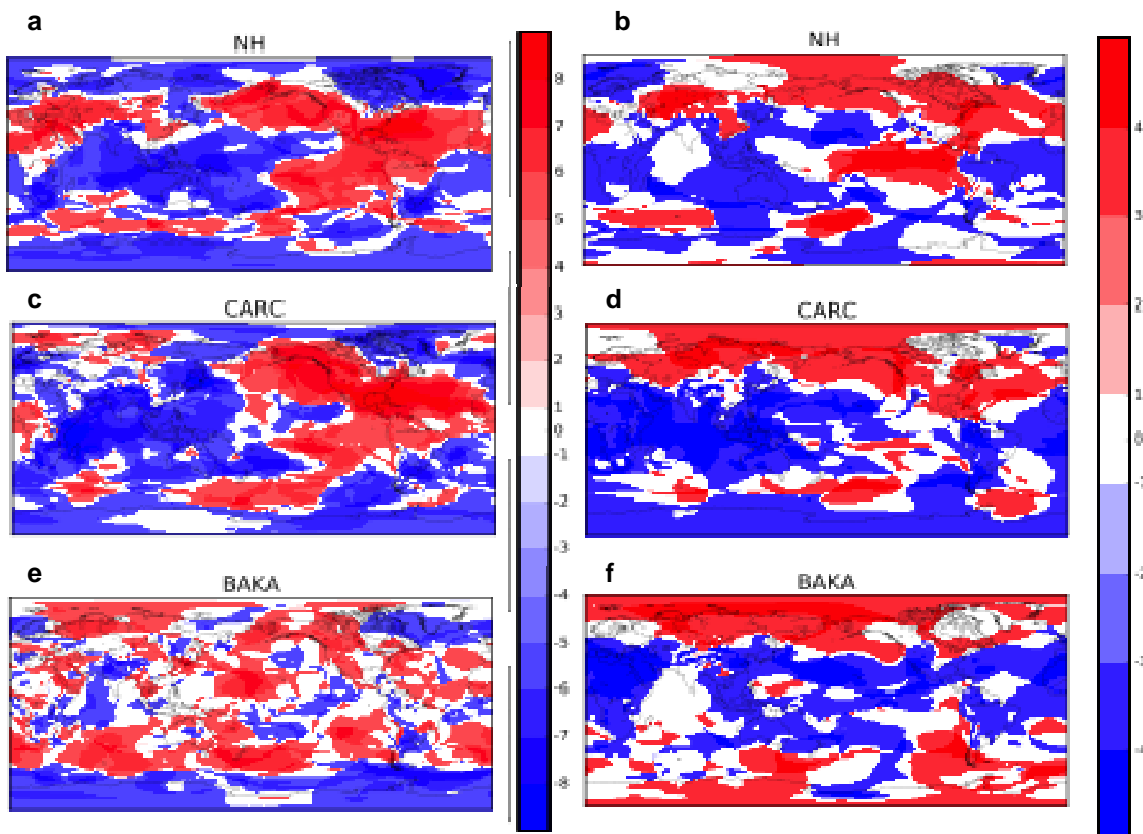


Figure 16: Left panels: Number of high resolution ocean models with the same positive (red) or negative (blue) correlation values between sea ice variations during the month of November over (a) NH, (c) CARC and (e) BAKA regions and next winter sea level pressure. Right panels: similar to left panels for low ocean resolution models.

3.2.6. Sea ice thickness modes of variability (BSC)

An increase of resolution in GCMs offers a valuable opportunity for improvement of the representation of physical processes as well as internal climate variability and externally forced climate response. We examined change in physically relatable patterns or modes of the Arctic sea ice variability on seasonal to interannual time scales (disentangled from a long-term climate change), manifested in sea ice thickness, as we increased nominal resolution from 1° to 0.25° . We used Nucleus for European Modelling of the Ocean model version 3.3.1 (NEMO3.3.1) with the embedded Louvain-la-Neuve sea Ice Model version 3 (LIM3) using single sea ice thickness category. Our NEMO-LIM3 setup is forced by the DFS4.3 surface forcing fields from 1958 to 2006 following the CORE bulk formulae. NEMO-LIM3 simulations are full-field initialized on 1 January 1958 from ensemble-mean of the ECMWF's Ocean Reanalysis System 4 (ORAS4) and the associated ensemble-mean sea ice reconstruction from BSC. We used a statistical framework for study of sea ice thickness anomalies based on the k-means clustering methodology after removing second order polynomial approximation of a long-term change in the Arctic. We found that the optimal number of Arctic sea ice thickness clusters is 3. This leads the k-means nonhierarchical method to the 3 patterns of sea ice thickness cluster centers and time series of cluster occurrences from 1958 to 2006 shown in Fig. 17 and Fig. 18.

Fig. 17 and Fig. 18 present three coherent and consistent Arctic sea ice thickness modes in both horizontal resolutions: Central Arctic Thinning (CAT) mode (cluster 1), Atlantic-Pacific Dipole (APD) mode (cluster 2), and Canadian-Siberian Dipole (CSD) mode (cluster 3). Monthly time series of Arctic sea ice thickness cluster occurrences in simulations with different resolutions show some regional differences, but overall large-scale structure and their persistence are compatible (reaching to inter-annual timescales). The pattern of CAT mode exhibits the highest level of inter-seasonal and inter-resolution variability (i.e., APD and CSD modes are more consistent among different resolutions and different seasons). ORCA1 (ORCA025) often has stronger amplitude of sea ice thickness mode anomaly patterns in winter (summer) than ORCA025 (ORCA1). Since we used the same surface forcing, DFS4.3 without any perturbation in forced ocean-sea-ice simulations at both horizontal resolutions, we anticipate that the analysis of future PRIMAVERA coupled simulations with different climate models over the longer period will likely reveal a stronger internal variability and possibly richer structure of sea ice thickness cluster patterns.

Sea ice thickness modes

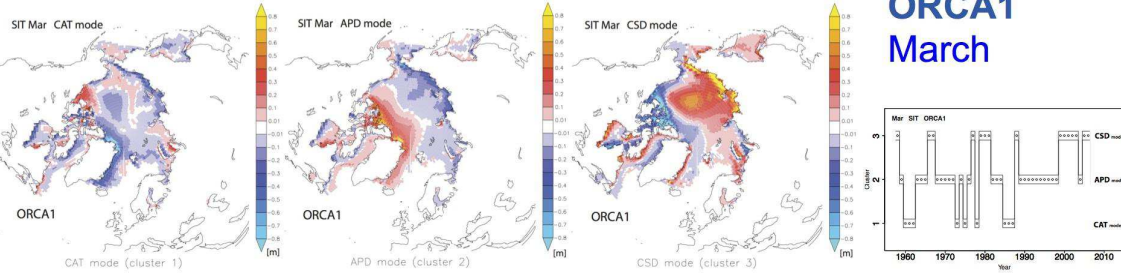
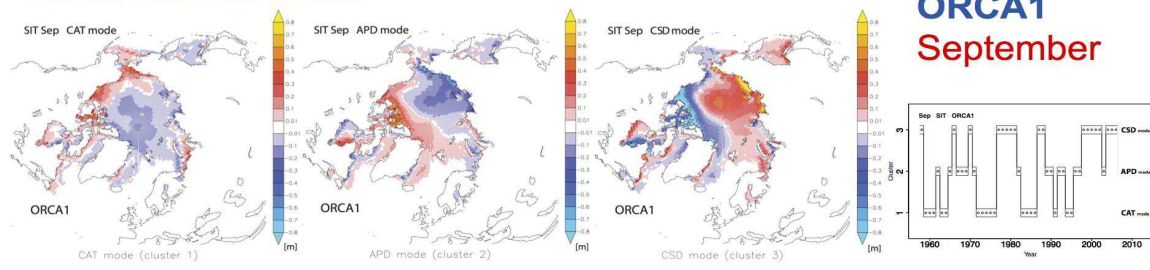


Figure 17: Patterns of Arctic sea ice thickness modes (CAT, APD and CSD) and their time series of occurrence in March in ORCA1L46 and ORCA025L75 configurations of NEMO3.3.1.

Sea ice thickness modes



Sea ice thickness modes

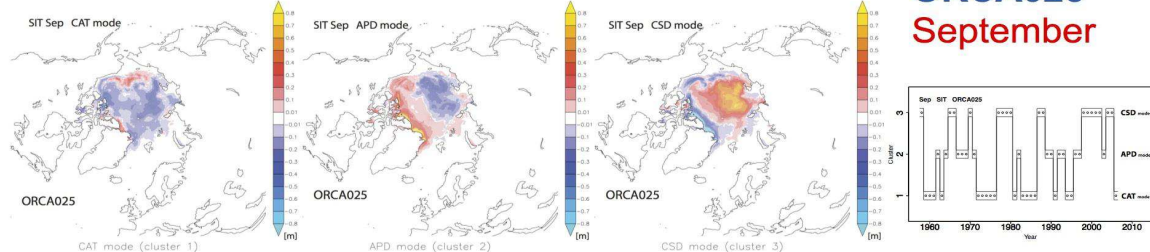


Figure 18: Patterns of Arctic sea ice thickness modes (CAT, APD and CSD) and their time series of occurrence in September in ORCA1L46 and ORCA025L75 configurations of NEMO3.3.1.

3.2.7. Sea ice extent (UCL)

March and September Arctic sea ice extents from all pre-PRIMAVERA simulations have been analyzed. Results generally show a decreased extent with higher resolution. Python scripts related to this diagnostic are also available on JASMIN.

Key findings for Arctic sea ice:

a) Results including multiple models:

- High resolution leads to a more realistic simulation of the Arctic sea ice concentration and might improve the realism of sea ice – atmosphere interactions (**SMHI**).
- Sea ice extent generally decreases with higher resolution across pre-PRIMAVERA runs (**UCL**).

b) Results including only one model (at different resolutions):

- The representation of vertical thermodynamic processes is unaffected by the increase in horizontal resolution using NEMO-LIM3.6 (**UCL / BSC**).
- Sea ice thickness increases with higher spatial resolution using NEMO-LIM3.6 forced by atmospheric reanalysis, due to higher heterogeneity in sea ice thickness and higher conduction fluxes (**UCL / BSC**).
- The ORCA1 (ORCA025) resolution with NEMO3.3.1-LIM3 often has a stronger amplitude of sea ice thickness mode anomaly patterns in winter (summer resp.) than ORCA025 (ORCA1 resp.) (**BSC**).

3.3. Atmosphere

3.3.1. Atmospheric blocking and eddy-driven jet variability (CMCC)

Atmospheric processes, such as atmospheric blocking and the eddy-driven jet variability in the North Atlantic domain, strongly interact with the North Atlantic Ocean and likely with the Arctic sea ice. In this regard, a preliminary analysis is under-way to assess the role of model resolution in the representation of such processes using an ensemble of pre-PRIMAVERA model runs currently available at JASMIN. The required data for this analysis (daily geopotential height at 500 hPa for the blocking and daily zonal wind at standard isobaric levels for the jet variability) are available for the following simulations: a single realization of the HadGEM3-GC2 (coupled model, MET-OFFICE) at two different resolutions and a single realization of the EC-EARTH-3.1 (atmosphere-only, CNR) at three different resolutions. A robust inference on the effect of increased model resolution would require at minimum a small ensemble of realizations. Despite this shortcoming, the analysis is performed aiming also to sharpen the tools and the methods applied in anticipation of the Stream-1 HighRes and LowRes simulations.

An example is provided in Fig. 19 for the wintertime blocking frequency along the Central Blocking Latitude, as in Athanasiadis et al. (2014). The differences in the climatological blocking frequency between different resolutions of the same model seem to be more consistent for the coupled model (HadGEM3-GC2) indicating an increase in blocking frequency with resolution. For the atmosphere-only model (EC-EARTH-3.1) the effect of increasing the resolution is rather elusive. In the absence of multiple realizations, sub-sampling the historical period can be used to assess the robustness of the above-mentioned differences. In this respect, the model assessment will be performed against both the ERA-Interim and NCEP/NCAR reanalyses as the respective climatologies exhibit non-negligible differences. The analysis discussed here is a preliminary step towards a more in-depth, multi-model assessment that will be performed on the Stream-1 simulations. Python scripts that compute the above-mentioned diagnostics have been uploaded to JASMIN.

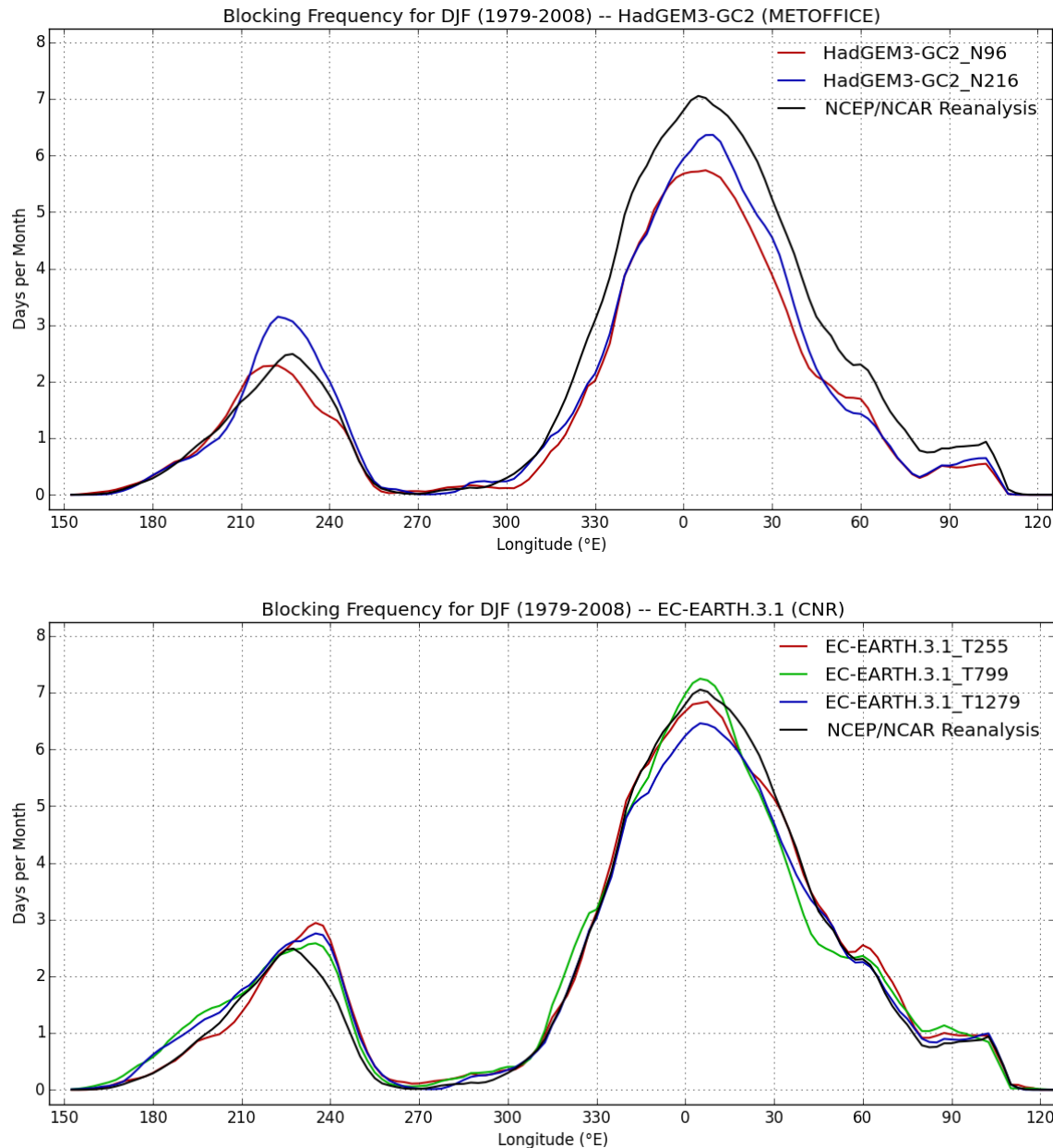


Figure 19: Frequency of occurrence of instantaneous blocking in wintertime (DJF) along the observed Central Blocking Latitude, as in Athanasiadis et al. (2014), for HadGEM3-GC2 (top panel) and atmosphere-only EC-Earth3.1 (bottom panel). Mean bias correction has been applied prior to the identification of blocking events as in Scaife et al. (2010).



3.3.2. Tropical cyclones and mid-latitude storms (MET OFFICE)

Some initial comparison of tropical and mid-latitude cyclones has been undertaken with the Met Office HadGEM3-GC2 and EC-Earth3.1 models at different resolutions (only these models since the code requires six hourly input data which only exists for these models). There are indications in both models that the Atlantic mid-latitude storm track has a stronger southerly branch as resolution is increased, hence agreeing better with reanalysis from ERA-Interim. For the tropical cyclones, both models show an increase in storm numbers from the lowest resolution model to the other models, but further analysis is needed (including using the ensemble members) to draw firm conclusions.

3.3.3. Rainfall and convection in Gulf Stream region (KNMI)

Using pre-PRIMAVERA EC-Earth AMIP simulations we have investigated the impact of model resolution on rainfall and convection in the Atlantic Gulf Stream region. This region is characterized by a strong SST front and is the main genesis region for cyclones over the North Atlantic. Two resolutions were compared, T159 (~150 km) and T799 (~25 km), for present day with prescribed daily SST's with 0.25° resolution. The analyses also included an extensive comparison with the available data sets. These analyses are described in Scher et al. (submitted, JAMES).

It is shown that mean precipitation increases with increasing resolution. Via an analysis of the position of the jet stream and other features of the large scale circulation, it is suggested that the differences in mean precipitation in the GCM are not caused by differences in large scale circulation, but mainly by local phenomena. Increasing resolution in the GCM especially leads to more extreme precipitation (Fig. 20). An assessment whether the increase in extreme precipitation deteriorates or improves model performance appears problematic as it depends on which observational product is used. Furthermore, 10 m wind convergence has been analyzed and it is shown that the higher resolution GCM shows more extreme wind convergence events and corresponds better to wind convergence derived from observations. Additionally, the number of deep convection events above the Gulf Stream increases with resolution in the GCM, enhancing the communication of SSTs up to the troposphere.

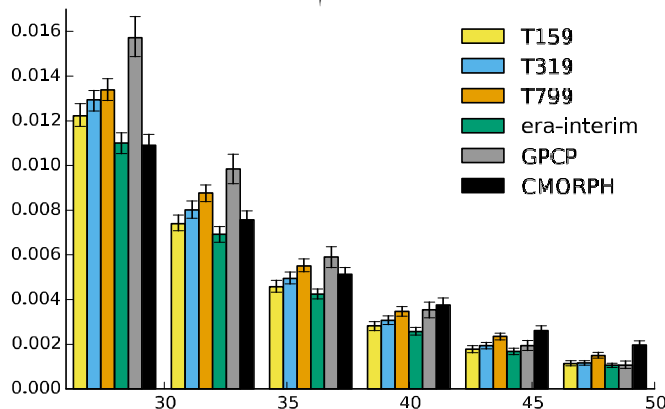


Figure 20: Distribution of wintertime daily rainfall events in the study area for EC-EarthT159/T319/T799, ERA-Interim (1985-2014) and GPCP 1dd observations (1997-2014). Each set of bars corresponds to the x-value at the center of the set of bars. The error bars indicate the 5-95% confidence interval estimated with bootstrapping daily event. From Scher et al. (submitted, JAMES).

3.3.4. SST smoothing in Gulf Stream region (KNMI)

To assess how differences in SST resolution affect rainfall, convection and storm development we have run the limited area model HARMONIE with 10 km resolution over the Gulf Stream region. The development of 27 past winter storms in the period 2006 to 2012 was investigated. Two experiments were compared: one with the observed SST field and one in which the SST field over the Gulf Stream region was smoothed. The development of the past storms was simulated realistically and significant differences in storm development were found due to the SST smoothing. The mechanisms responsible for this have been analyzed. A paper has been submitted to JGR-Atmospheres (Scher et al., submitted, JGR).

The response of storms to decreased SST-gradients is caused by changes in latent heat flux and by changes in the temperature structure of the atmosphere. The former strengthens (weakens) storms north (south) of the SST-front, where SSTs get warmer (colder) when decreasing SST-gradients. The latter weakens all storms. In the South, both act the same direction and all storms weaken. In the North they act in opposite directions, and about half of the storms weakens, the other half strengthens. Results are presented in Fig. 21.

The original plan was to investigate the impact of smoothed SSTs in EC-Earth AMIP simulations. However, serious problems with respect to the smoothing were encountered during the initial analyses. Therefore, these experiments have been first performed with the limited area model HARMONIE in order to guide the analyses of the smoothed EC-Earth AMIP SST experiment. The gained understanding will now be applied to the Stream 1 PRIMAVERA runs.

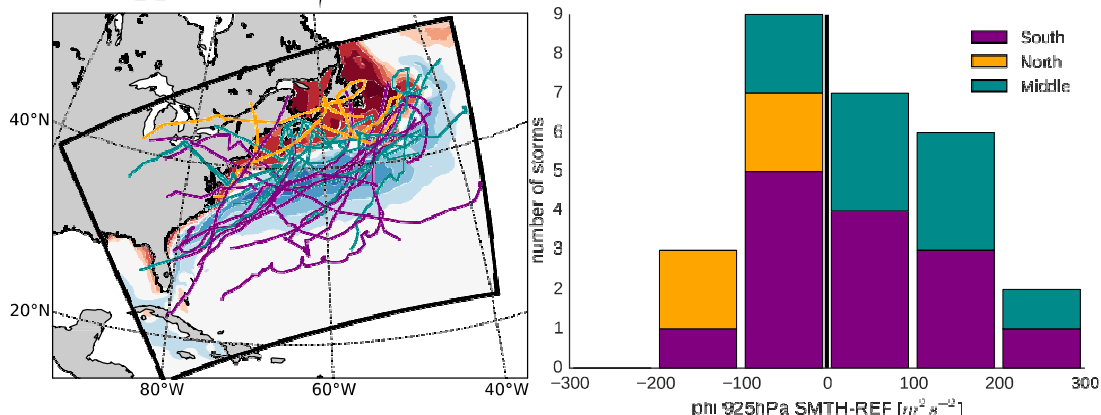


Figure 21: Left: Tracks of the simulated storms. Yellow (purple) lines denote tracks that are on average north (south) of the SST-front. Blue lines denote tracks that are aligned along the front. Contours: difference of SSTs of smoothed (SMTH) and reference (REF) runs (SMTH-REF) averaged over study period (NDJF 2006-2012). The black box denotes the domain of the regional simulation. Right: Differences in geopotential height of the 925 hPa surface between the SMTH and the REF runs averaged in a box of 30x30km around the track, coloring same as in the left hand panel. From Scher et al. (submitted, JGR).

3.3.5. 2m-temperature bias (AWI)

The ocean component of AWI-CM - FESOM (Wang et al., 2014) uses unstructured meshes, which allows using variable resolutions without traditional nesting. Despite of the flexibility of unstructured meshes, one needs to carefully design meshes so that the variable resolution can most efficiently improve the simulated results with least possible computational cost. We proposed a new approach to set up variable resolution, which uses the satellite-observed sea surface height variability to determine the regions where high resolution should be assigned (Sein et al., 2016). This approach is verified using both idealized experiments and ocean simulations. It will also become one of the standard mesh design methods for general FESOM users. The added value of the use of the high resolution ocean model was demonstrated by running two different FESOM ocean setups coupled with ECHAM6 atmospheric model.

The first one employs a coarse mesh with nominal resolution of about 1° in the global ocean, about 25-km north of 50°N, about 1/3° in the equatorial band, and moderate refinement along the coasts. This setup is further referred to as LR (Fig. 22, upper panel).

The second setup uses a locally eddy-resolving mesh. Its design relies on the AVISO satellite altimetry product. The coarsest resolution on this mesh is set to ~60 km, and the finest resolution is ~10 km. The refinement was determined by a low-pass filtered SSH variance (SSHV) pattern derived from the AVISO data. Fine resolution is obtained in regions with high SSHV, including the pathways of main currents - the Gulf Stream, Kuroshio, Antarctic Circumpolar Current (ACC) and Agulhas Current. This setup is referred to as HR (Fig. 22, lower panel). The mesh contains about 1.3×10^6 surface grid nodes, which is close to the number of nodes on a Mercator 1/4° mesh (only wet nodes are dealt with on

unstructured meshes). This mesh size was also selected to ensure reasonably fast simulations with available computational resources.

The simulations with two global ocean setups of AWI-CM were carried out according to the PRIMAVERA protocol. Ocean model was initialized with 1950-1954 mean winter EN4 data, then 50 years coupled spin-up with 1950 forcing was performed. After the spin-up both the LR and HR AWI-CM models were run with CMIP5 20 century forcing from 1950 till 2005. Figure 23 clearly demonstrates the added value in 2m temperature. The biases are strongly reduced almost over the entire globe. The most remarkable reduction can be seen in equatorial Pacific, Kuroshio current and Southeast Asia.

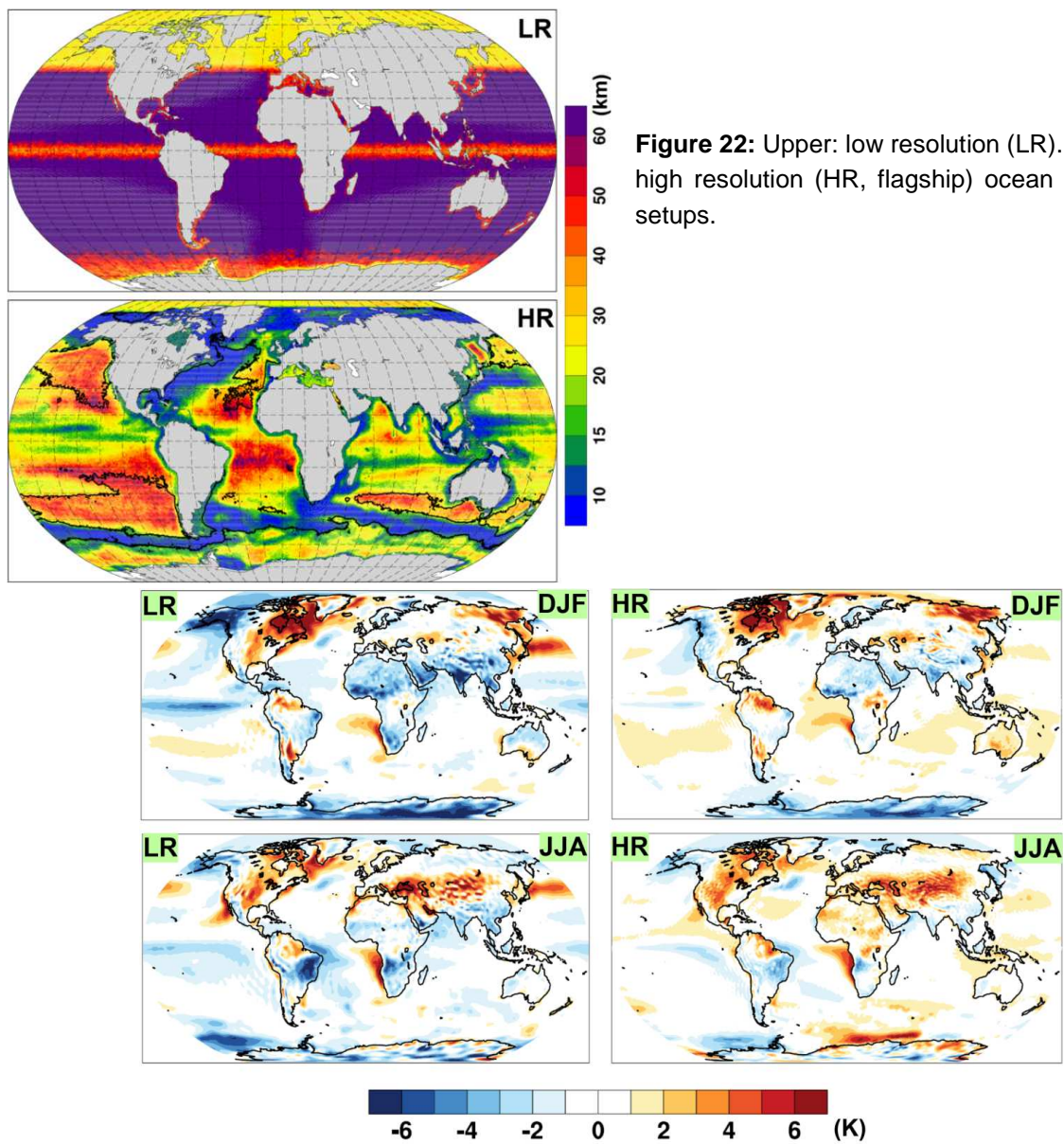


Figure 22: Upper: low resolution (LR). Lower: high resolution (HR, flagship) ocean models setups.

Figure 23: 1980-2000 mean DJF (upper) and JJA (lower) 2m temperature bias (Model – ERA-Interim). Left: low resolution, right: high resolution (flagship) simulations.

3.3.6. European extreme precipitation and its response to large-scale atmospheric circulation variability (UREAD)

The effects of atmospheric modes of variability, such as the North Atlantic Oscillation (NAO), on the spatiotemporal distribution of European mean precipitation are relatively well-documented, but less is known about their impact on precipitation extremes. It is important to determine how well GCMs represent relationships between extremes and large-scale variability, particularly for understanding the implications of a given medium-range or seasonal NAO forecast for extreme precipitation.

In this context, we are evaluating the resolution sensitivity of European extreme precipitation in gridded observations (ECA&D E-OBS) and in an ensemble of both atmosphere-only and coupled global simulations, compiled as part of the EU Horizon2020-funded PRIMAVERA project, where mid-latitude horizontal resolution is increased from ~135 to ~25km. The global models comprising this study are HadGEM3-GA3, -GA6, -GA7, and EC-Earth3.1 (atmosphere-only), and HadGEM3-GC2, EC-Earth3 and CNRM-CM5 (coupled).

A multi-metric model evaluation is performed to: (i) compute extreme quantile composites for NAO+ and NAO- regimes; (ii) apply generalized extreme value analysis to daily precipitation and aggregate results over large European river basins ($>50000 \text{ km}^2$); and (iii) determine the contribution to extreme precipitation from phenomena whose frequency is impacted by large-scale variability, such as (Euro-Atlantic sector) extratropical cyclones.

For example, the 95th percentile of daily winter precipitation was composed (NAO+ - NAO-) and zonally averaged (Fig. 24). The large-scale pattern – wet north-western Europe and dry southern Europe – is reproduced by HadGEM3-GA3. However, the response of extreme precipitation between ~40-50°N to NAO phase is overestimated across the resolution hierarchy and the variability between 58-65°N is captured only at N512 resolution, likely due to its better representation of Norwegian topography.

Complementary statistical and process-based model evaluations aim to characterise (and evaluate the resolution sensitivity of) relationships between large-scale atmospheric variability and European extreme precipitation.

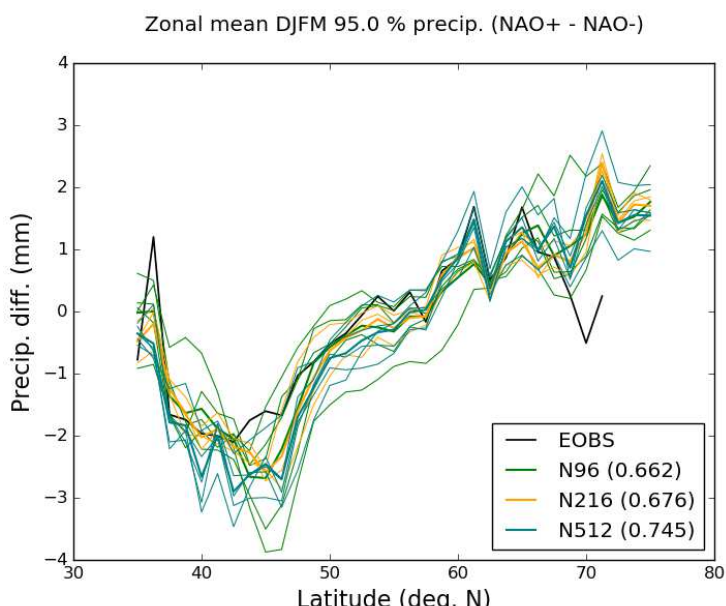


Figure 24: Zonal mean (-40-60 °E) difference between European extreme (95th percentile) winter precipitation (December-March) under NAO+ vs NAO- in gridded observations (EOBS) and HadGEM3-GA3.0 simulations (UPSCALE campaign), with horizontal resolutions of ~130km (N96), ~60km (N216) and ~25km (N512). Precipitation over land only. Values in legend give ensemble mean root-mean-square error (model-EOBS).

3.3.7. Global water cycle (UREAD)

Demory et al. (2014) have demonstrated that the global water cycle is sensitive to global climate model (GCM)'s horizontal resolution, up to about 60 km, where the results converge. While ocean precipitation decreases with higher resolution, land precipitation increases due to higher moisture convergence over land. The contribution of moisture transport to land precipitation also increases, whereas moisture recycling, a quantity that is known to be overestimated by state-of-the-art GCMs, tends to decrease. One question that came out of this study is whether such mechanisms are model dependent.

In this study, we are computing energy and water budgets in an ensemble of atmospheric models made of pre-PRIMAVERA simulations (HadGEM3-GA3 and EC-EARTH3.1) and complemented by simulations from three additional GCMs (MRI3.2, CAM5.1, GFDL-HiRAM) in order to investigate systematic changes with resolution and propose physical mechanisms responsible for hydrological processes sensitivity to resolution.

We produced Trenberth type diagrams for each model to help visualise energy and water budget changes with resolution. Whenever possible, depending on high-frequency data availability, the total moisture transport is further decomposed into the contributions of mean circulation and transient eddies. The sensitivity of these different terms to resolution and their contribution to the mean precipitation are assessed at the global scale, in the tropics and mid-latitudes, and over each continent taken separately. A decomposition into orographic and non-orographic precipitation is also carried out. Additional sensitivity experiments with different resolution of orography have been analyzed to assess independently the role of orography (HadGEM3-GA6).

Our results show that: (1) in all models, there is an increase of moisture transport to land when the resolution of the atmospheric model is increased, but the increase in grid-point models is more than twice that of spectral models; besides the fraction of land precipitation tend to increase in grid-points models and decrease in spectral models (Fig. 25); (2) the response is largely dominated by the tropics and the advection of moisture by the mean circulation; (3) at the global scale, the increased moisture transport balances the increase of orographic precipitation (which amount is larger in grid-point models with better resolved reliefs); (4) at the regional scale, several systematic improvements are found which can be linked to a better simulated seasonal mean circulation.

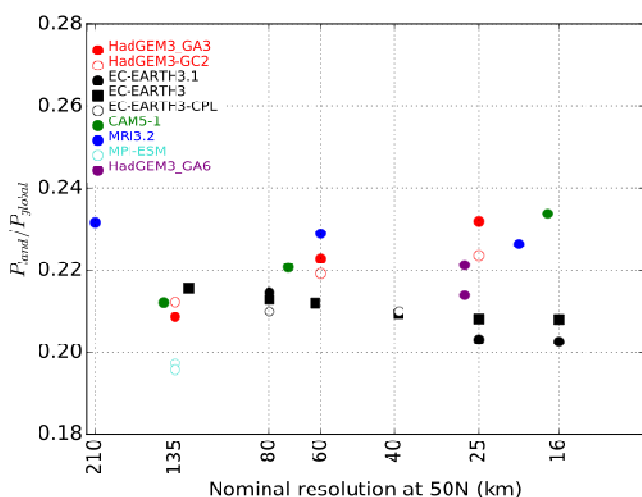


Figure 25: Ratio of land to global precipitation as a function of model resolution at 50°N. Plain circles stand for atmosphere-only experiments and open circles for coupled experiments.

- ▶ It is interesting to note that two different behaviours arise depending on model formulation: in grid-point models (HadGEM3, CAM5-1), the land to global precipitation ratio increases with resolution whereas it decreases in spectral models (EC-Earth3, EC-Earth3.1, MRI3.2).
 - ▶ Coupling does not modify this behaviour.
- The purple circles stand for two experiments testing the sensitivity to the resolution of orography: the control (top) uses HadGEM3-GA6 on grid N480, the perturbed experiment (bottom) uses the same atmospheric resolution but N96 orography.

Key findings for Atmosphere:

a) Results including multiple models:

- Increasing atmosphere resolution with HadGEM3-GC2 leads to an increase in blocking frequency, while no trend is observed with the atmosphere-only EC-Earth3.1 model (**CMCC**).
- The Atlantic mid-latitude storm track has a stronger southerly branch as resolution is increased in HadGEM3-GC2 and EC-Earth3.1, hence agreeing better with reanalysis from ERA-Interim (**MET OFFICE**).
- Increased resolution leads to an increase in storm numbers for HadGEM3-GC2 and EC-Earth3.1 (**MET OFFICE**).
- Moisture transport to land increases when atmospheric resolution increases, with a higher increase (more than twice) for grid-point models compared to spectral models and an increase (decrease) of the fraction of land precipitation in grid-point (spectral respectively) models (**UREAD**).

b) Results including only one model (at different resolutions):

- According to EC-Earth AMIP simulations, there is an increase of extreme precipitation and deep convection with increasing resolution over the Gulf Stream region. The improvement of increasing resolution on extreme precipitation and deep convection is mainly due to a better representation of local processes and not due to a better simulation of the large scale circulation (**KNMI**).
- Smoothing of SST with HARMONIE model decreases baroclinic instability, but can increase or decrease the latent heat flux depending on the storm track. These two mechanisms can therefore reinforce or counteract each other. The consequence is that weakening as well as strengthening of storms can occur due to smoothing of SSTs (**KNMI**).
- The 2m temperature biases are strongly reduced almost over the entire globe using the high-resolution AWI-CM model with FESOM ocean model. The most remarkable reduction can be seen in equatorial Pacific, Kuroshio current and Southeast Asia (**AWI**).
- The response of extreme precipitation between ~40-50°N to NAO phase is overestimated across the resolution hierarchy of HadGEM3-GA3 (atmosphere-only model) and the variability between 58-65°N is captured only at higher (N512) resolution, likely due to its better representation of Norwegian topography (**UREAD**).

3.4. Peer-reviewed articles arising from the project

Published articles:

- Milinski S., Bader J., Haak H., Siongco A. C., Jungclaus J. H. (2016). High atmospheric horizontal resolution eliminates the wind-driven coastal warm bias in the southeastern tropical Atlantic. *Geophysical Research Letters*, doi: 10.1002/2016GL070530.
- Roberts M. J., Hewitt H. T., Hyder P., Ferraira D., Josey S. A., Mizielinski M., Shelly A. (2016). Impact of ocean resolution on coupled air-sea fluxes and large-scale climate, *Geophysical Research Letters*, doi: 10.1002/2016GL070559.
- Sein D. V., Danilov S., Biastoch A., Durgadoo J. V., Sidorenko D., Harig S., Wang Q. (2016). Designing variable ocean model resolution based on the observed ocean variability. *Journal of Advances in Modeling Earth Systems*, doi: 10.1002/2016MS000650.

Submitted articles:

- Scher S., Haarsma R. J., de Vries H., Drijfhout S. S., van Delden A. J. (submitted). Resolution dependence of precipitation and deep convection over the Gulf Stream. Submitted to JAMES.
- Scher S., Haarsma R. J., de Vries H., Drijfhout S. S., van Delden A. J. (submitted). Development of mid-latitude storms sensitive to SST-gradients. Submitted to JGR-Atmospheres.

Articles in preparation:

- Docquier D., Massonnet, F., Tandon, N. F., Lecomte, O., Fichefet, T. (in preparation). The Arctic sea ice drift-strength feedback modeled by NEMO-LIM3.6.
- Exarchou E. et al. (in preparation). Impact of resolution in oceanic heat pathways in global climate models.
- Grist J. et al. (in preparation). Coupled model resolution dependence of heat transport and surface fluxes.
- KNMI (in preparation). Publication on impact of resolution on precipitation on PRIMAVERA stream 1 simulations.
- KNMI (in preparation). Publication on impact of SST smoothing in EC-Earth and HighResMIP targeted simulations (smoothed-SST, see for HighResMIP simulations: Haarsma et al. 2016).
- Koenigk T. et al. (in preparation). The impact of high resolution in global coupled models on the representation of deep water formation in the North Atlantic.
- Fuentes Franco et al. (in preparation). The impact of high resolution in global coupled models on the representation of Arctic sea ice and sea ice – atmosphere interactions.
- Massonnet F. et al. (in preparation): Importance of sea ice thickness distribution for the representation of ice growth.
- UREAD (in preparation). Publication on sensitivity of the hydrological cycle to global climate models' resolution.

3.5. Other references

- Athanasiadis P. J., Bellucci A., Hermanson L., Scaife A. A., MacLachlan C., Arribas A., Materia S., Borrelli A., Gualdi S. (2014). The representation of atmospheric blocking and the associated low-frequency variability in two seasonal prediction systems. *Journal of Climate*, doi: 10.1175/JCLI-D-14-00291.1.
- Brodeau L., Koenigk T. (2016). Extinction of the northern oceanic deep convection in an ensemble of climate model simulations of the 20th and 21st centuries. *Climate Dynamics*, doi: 10.1007/s00382-015-2736-5.
- Demory M.-E., Vidale P. L., Roberts M. J., Berrisford P., Strachan J., Schiemann R., Mizienlinski M. (2014). *Climate Dynamics*, doi: 10.1007/s00382-013-1924-4.
- Eastwood S., Larsen K R., Lavergne T., Nielsen E., Tonboe R. (2011). Global sea ice concentration reprocessing: product user manual, product OSI-409. Version 1:3.
- Haarsma R. et al. (2016). High Resolution Model Intercomparison Project (HighResMIP v1.0) for CMIP6. *Geoscientific Model Development*, doi: 10.5194/gmd-9-4185-2016.
- Hewitt H. T., Roberts M. et al. (2016). The impact of resolving the Rossby radius at mid-latitudes in the ocean: results from a high-resolution version of the Met Office GC2 coupled model. *Geoscientific Model Development*, doi: 10.5194/gmd-2016-87.
- Holte J., Gilson J., Talley L., Roemmich D. (2010). Argo mixed layers. Scripps Institution of Oceanography/UCSD p. <http://mixedlayer.ucsd.edu>. Accessed Jan 2015.
- Koenigk T., Caian M., Nikulin G., Schimanke S. (2016). Regional Arctic sea ice variations as predictor for winter climate conditions. *Climate Dynamics*, doi: 10.1007/s00382-015-2586-1.
- Minobe S., Kuwano-Yoshida A., Komori N., Xie S. P., Small R. J. (2008). Influence of the Gulf Stream on the troposphere, *Nature*, doi: 10.1038/nature06690.
- Olason E., Notz D. (2014). Drivers of variability in Arctic sea-ice drift speed. *Journal of Geophysical Research*, doi: 10.1002/2014JC009897.
- Reynolds R. W., Rayner N. A., Smith T. M., Stokes D. C., Wang W. (2002). An improved in situ and satellite SST analysis for climate. *Journal of Climate*, doi: 10.1175/1520-0442(2002)015<1609:AIISAS>2.0.CO;2.
- Scaife A. A., Woollings T., Knight J., Martin G., Hinton T. (2010). Atmospheric blocking and mean biases in climate models. *Journal of Climate*, doi: 10.1175/2010JCLI3728.1.
- Von Storch J.-S., Haak H., Hertwig E., Fast I. (2016). Vertical heat and salt fluxes due to resolved and parameterized meso-scale eddies. *Ocean Modelling*, doi: 10.1016/j.ocemod.2016.10.001.
- Wang Q., Danilov S., Sidorenko D., Timmermann R., Wekerle C., Wang X., Jung T., Schröter J. (2014). The Finite Element Sea Ice-Ocean Model (FESOM) v.1.4: formulation of an ocean general circulation model. *Geoscientific Model Development*, doi: 10.5194/gmd-7-663-2014.

4. Lessons Learnt

Positive lessons:

- A wide range of analyses has been carried out using all pre-PRIMAVERA model outputs, which shows the benefits from using multiple models. For example, we showed that increased northward heat transport with higher ocean resolution is a robust feature across all global climate models.
- Some key results related to the impact of resolution have been found. For example, increasing ocean resolution from 1° to $1/4^{\circ}$ does not show any significant difference in the precipitation structures compared to observations, while the use of $1/12^{\circ}$ ocean resolution with a higher atmosphere resolution clearly allows a better representation.
- There are clear benefits from working across modeling centers in the EU, including discussions about results and share of work and perspectives.

Negative lessons:

- Not all pre-PRIMAVERA models provide the necessary frequency (hourly, daily, etc.) and the time period needed for accurately computing diagnostics (e.g. sea ice drift-strength feedback), which reduces the model samples for analysis. Fortunately, this drawback will be resolved in the PRIMAVERA Stream 1 simulations where all models will provide the standardized CMIP6 model outputs.
- Different versions of the same model provide model outputs on JASMIN, which makes the comparison more difficult (e.g. it is sometimes not easy to see if differences are due to resolution or to model version difference).
- Increasing horizontal resolution does not systematically improve the results and conclusions are process-dependent. When no improvement is detected, it should be reminded that high-resolution simulations have generally undergone less tuning than standard resolution simulations (or no tuning at all) and may still use parameterizations optimized for coarser resolutions. This effect has not been quantified in these studies.

Neutral lessons (neither negative nor positive):

- As model resolution increases, and models become better able to represent climate processes, typical analysis techniques have greatly increased requirements for data input, either from higher temporal or spatial (or both) frequency. This makes the analysis more challenging, and platforms like JASMIN become more vital.
- One of the main lessons learnt so far is the crucial importance of careful design of computing intensive simulations. Test simulations on which the proposed analyses can be performed are in this respect a necessary step in the design process.



5. Links Built

- WP2 worked closely together with WP1 on the development of diagnostics and metrics. Many of the WP2 model diagnostics have their equivalent WP1 metric.
- These diagnostics will also be available for application for model simulations in WP3, WP4 and WP5. For example, the air-sea coupling work will have strong links between WP2 and WP4, the latter providing the multi-model eddy-resolving coupled simulations.
- Links were built with the proposed activities and targeted experiments in HighResMip, e.g. with the smoothed SST experiments.